the double-stranded replicative form. Nevertheless, such RNA, if any, trapped in membranous structures of the cells may not be conferred resistance to nucleases. In the RFB system, RNase-resistant HCV RNA was not detected after transfection of mutant clones (described later). Furthermore, in cells harvested on day 110 p.t., negative-strand HCV RNA was detected by tagged RT-PCR (Fig. 2D).

To verify that this system supports the replication of transfected HCV RNA, we constructed two mutated full-length HCV RNAs, termed H77cHel− and H77cRdRp−, containing lethal mutations of helicase and polymerase, respectively. After transfection, the residual RNA of these mutant clones gradually declined in the culture fluid, and no RNA was detected by RT-PCR after day 38 and 40 p.t., for H77cHel− and H77cRdRp−, respectively (Fig. 2A, H77cHel−: open triangles; H77cRdRp−: filled circles). Thus the detection of HCV RNA 44 days after transfection of wild-type HCV RNA must have been due to actual viral replication.

To confirm HCV replication and to determine whether mutations arose during the course of the study, we determined the nucleotide sequences of entire nonstructural regions of the clone detected on day 110 p.t. and compared them with the original clone (Fig. 2E). We observed 43 substitution mutations, all of which resulted in amino acid changes. This is not derived from RT errors during RT-PCR amplification because similar sequence changes were seen in the independent RT-PCR reaction. In particular, mutations of V1700S in the NS4A, E1937G in the NS4B, and K1298N in the NS3 regions were frequently observed (in 60% or more of the sequenced clones), which suggests that these mutations might enhance RNA replication within the FLC4-RFB system. We are now analyzing whether or not transcripts with these mutations enhance infectivity or have a replication advantage in RFB culture.

Late-stage culture fluid (80 to 110 days posttransfection) was collected, concentrated, and examined by TEM. A number of spherical particles, between 30 and 80 nm in diameter, were observed, and probably represent two entities of approximately 30 and 60 nm in size (Fig. 3A). The suspension was then fractionated by spinning within a continuous 10–60% (w/w) sucrose gradient. The fractions were then treated with Triton X-100/NaOH/polyethylene glycol and assayed for HCV core protein. The core protein was detected in both 1.07 and 1.20 g/ml fractions, while HCV RNA was predominantly detected in fractions of 1.03–1.09 g/ml (Fig. 3B). Although quantitative assays to detect HCV envelope proteins have not been developed, the lower density fraction observed in this study (1.03–1.09 g/ml) might reflect the presence of HCV particles (1.03–1.12 g/ml), as previously observed in the serum of hepatitis C patients (Kanto et al., 1994; Kaito et al., 1994). The higher density fraction, in contrast, may represent empty particles without RNA. To distinguish between the particles observed in these fractions, an indirect immunogold electron microscopic study was carried out (Figs. 3C and D). Spherical virus-like particles, 55 to 60 nm in diameter, in the 1.07 g/ml fraction reacted with monoclonal antibody to HCV E1 protein. We did not observe any specific reactions of concentrated supernatant from transfected cells with anti-Histidine antibody (Fig. 3E).

The secondary passage

The virus particle-containing supernatant collected at days 93, 94, and 95 p.t. was pooled and transferred to a fresh RFB culture of FLC4 cells. No HCV RNA was detected in supernatant collected at days 1–16 p.i. However, HCV RNA was detected on day 18, 24, and 28 p.i. The HVR sequences of this HCV RNA were mostly (90%) A1 clone sequences. New clones with a single base change were detected after another 14 days. In addition, HCV core protein was detected in the culture fluid on day 24 and 28 p.i. (Table 3). These results further suggest that HCV is produced in RFB culture and that released HCV is infectious.

Discussion

Despite numerous efforts to grow HCV, full replication of HCV has not been achieved in conventional monolayer cultures using any type of cell (Kato and Shimotohno, 1999; Thomson and Liang, 2000). Even when HCV RNA is detected by PCR in monolayer cultures, synthesis of newly synthesized HCV-specific proteins is not observed (Bartenschlager and Lohmann, 2001). A robust and reliable cell-culture system by which to grow HCV is urgently needed (Randall and Rice, 2001).

Recent reports have demonstrated HCV replication in human hepatocytes following transplantation into mice (Ilan et al., 2002; Mercer et al., 2001). This model provided a useful system to evaluate anti-HCV agents. However, researchers have yet to isolate infectious HCV virions.

In this connotation, the establishment of a HCV replication system (engineered HCV minigenomes) has been a real breakthrough in recent HCV research (Lohmann et al., 1999; Blight et al., 2000). This has also made reverse genetic HCV research possible. Furthermore, the ability to passage these cells has revealed that clones with "adaptive" mutations eventually become dominant (Blight et al., 2000; Lohmann et al., 2001; Krieger et al., 2001). However, the consensus sequences responsible for enhancement of HCV RNA replication have not been identified, even after examinations of the same clone (type 1b) and hepatocyte cell line (Huh-7 cells). This system was first developed to replicate only the nonstructural region of HCV genome, but further developed to enable replication of the full-length HCV genome. Although HCV RNA was synthesized, along with all properly processed HCV proteins, infectious virions were not produced (Ikeda et al., 2002; Pietschmann et al., 2002). Host cell factor(s) essential for virus assembly and release might not be provided, even by Huh-7 cells, which

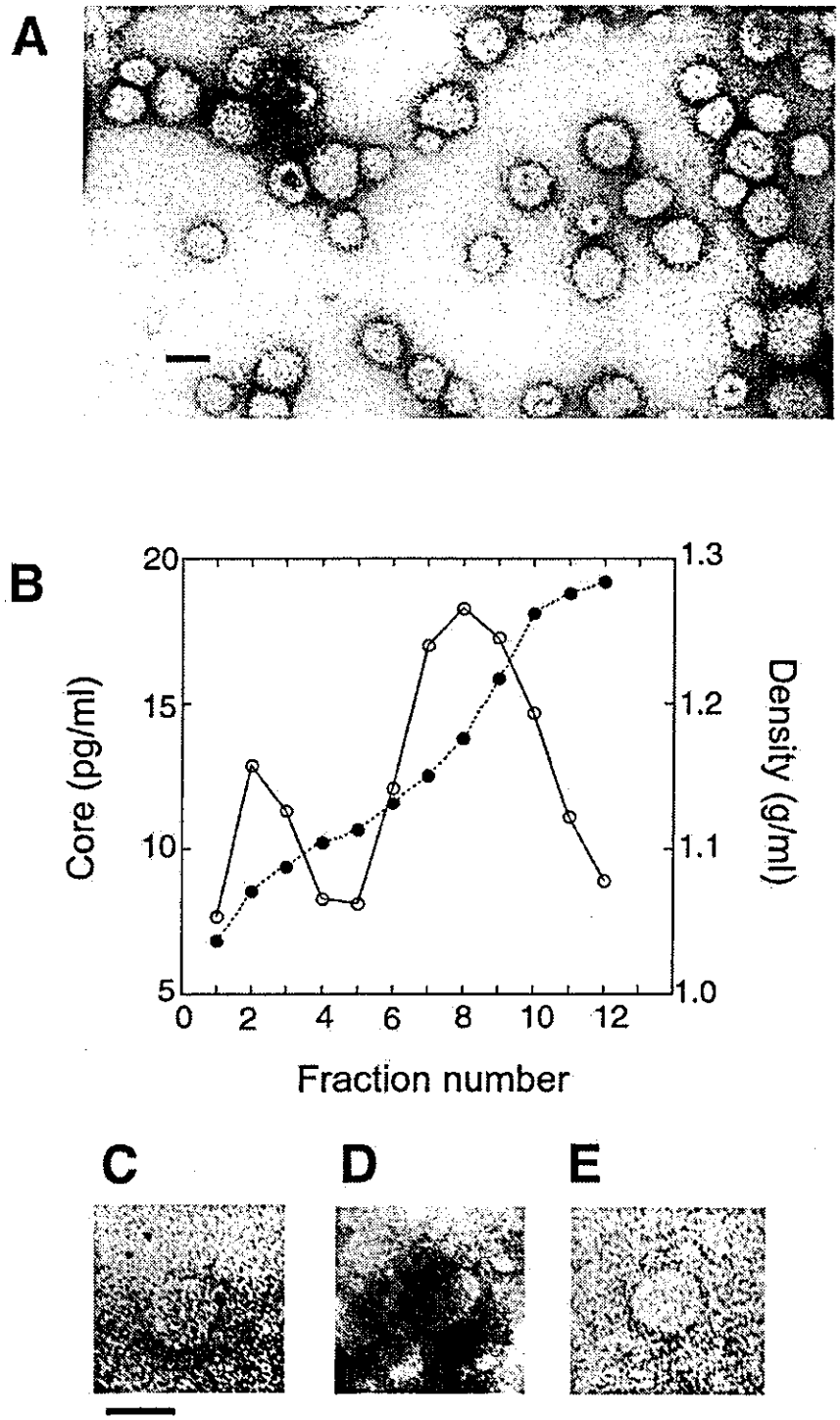

Fig. 3. Analysis of HCV-like particles in culture medium. (A) Culture fluid of the H77c transfectant was concentrated, stained with uranyl acetate, and examined by TEM. (B) HCV core protein in fractions from sucrose density gradient centrifugation. Amounts of HCV core protein (O) and buoyant densities (●) are shown. (C, D, E) Immunoelectron microscopy of the particles purified by sucrose gradient centrifugation. (C, D) Virus-like particles reacted with mouse monoclonal antibody against HCV E1 protein at a dilution of 1:10, and their antibody haloes were identified by binding to goat anti-mouse IgG-conjugated colloidal gold particles (6 nm) at a dilution of 1:20. (E) Control reaction using mouse monoclonal antibody against histidine residues antigen. The scale bars represent 50 nm.

Table 3
Secondary passage of HCV produced from the viral RNA transfection in the RFB culture

Days	HCV RNA[a]	Core[b] (pg/day)
−2	−	0
0[c]	+	5.3
1	+	2.1
3	−	0
5	−	0
7	−	0
9	−	0
11	−	0
13	−	0
16	−	0
18	+	0
20	−	0
22	−	0
24	+	6.9
28	+	14.5

[a] HCV RNA was detected qualitatively by RT-PCR (positive, +; negative, −).
[b] Core antigen was measured by the EIA method.
[c] Supernatant fluid of the RFB culture transfected with HCV RNA was transferred to new FLC4 cells in the RFB on day 0.

are capable of hosting viral RNA replication and HCV protein synthesis.

The results presented in this article clearly indicate that HCV replicates in FLC4 cells in the RFB system. In this study, we repeated the infection, transfection, and secondary passage experiments three times and obtained reproducible results. We also performed a mock-infected RFB culture for 4 months, during which time culture supernatant was harvested every week and examined for HCV RNA and HCV core protein. Negative results were obtained for both (data not shown).

In the culture medium of FLC4 cells in RFB culture, 10^6 – 10^7 copies/day of HCV were detected 2–3 weeks after infection, and 10^5 – 10^6 copies/day were detected 2–4 months after transfection. Although the viral growth of HCV in culture remains inefficient compared to that of other known viruses, this is the first report to unequivocally demonstrate HCV replication in tissue culture, as well as the production of infectious HCV derived from full-length HCV RNA.

The reason for different profiles of detection of HCV RNA and core protein is unclear (Fig. 2B). It is possible that the two assays have different sensitivities. Differences in the half-lives of viral RNA and HCV core protein may be also explain the difference. Nonetheless, the slow but gradual increase in HCV RNA and core protein observed in this study excludes the possibility that the results are due to HCV contamination or detection of the originally infused HCV RNA. These results also suggest that selection of clones capable of viral replication occurs during FLC4/RFB culture. Furthermore, it was shown that the viral quasispecies have changed before and after passages. Efforts to select clones with adaptive mutations enhancing both RNA replication and the production of infectious progeny are ongoing.

The key point of this work is the RFB culture, which allows liver cells to maintain their physiological function for a long time in culture. The RFB is a vertically extended cylindrical matrix with porous bead microcarriers having a honeycomb-like structure. This structure enables contact between cells and circulating components, including oxygen and nutrients, without excessive shear stress. The RFB has an effective air space ratio of 50%; thus, the microcarriers have much of their surface area exposed, which supports the long-term viability of the cells in culture. Cells cultured in the RFB system maintain their polarity within a well-defined 3D structure, having tight intercellular junctions and close connectivity with other epithelial cell membranes. These characteristics are important for the sustained function of liver cells in culture, including secretory and endocytic/transcytotic hepatocyte pathways.

A number of enveloped viruses have been reported to mature at distinct membrane domains within monolayers of polarized epithelial cells. For example, paramyxoviruses and orthomyxoviruses bud from the apical surface, while rhabdoviruses, retroviruses, and baculoviruses bud from a basolateral domain (Boulan and Sabatini, 1978). Similarly, FLC4 cells in the RFB are thought to maintain their polarity in a well-defined 3D structure, which is necessary for the replication and secretion of HCV.

The use of FLC4 cells may contribute to the success of this system. We have previously shown that this cell line supports efficient HCV structural gene expression by a recombinant adenovirus vector (Aoki et al., 1998). The results of this report also suggest that some host factors which increase the efficiency of translation of HCV minigene RNA are present in FLC4, but not other cells, including several commonly used human hepatoma cell lines. Furthermore, using a cell fusion assay, we recently found that FLC4 cells exhibit a high affinity for cell fusion with CHO cells expressing HCV envelope proteins on their surface (Takikawa et al., 2000). However, FLC4 cells in conventional monolayer cultures were not observed to support HCV replication following infection with no. 6 plasma. Although a small amount of virus was detected by PCR on day 19 p.i., less than 1 to 10–100th of the amount of virus per cell obtained with RFB culture was observed (data not shown). HCV RNA was not detected beyond day 19 p.i.

We are now attempting to simplify the method of RFB culture, by culturing fewer cells to better monitor HCV replication and intracellular events. In the immediate future, we will attempt to confirm the infectivity of HCV isolated from RFB culture by inoculation of chimpanzees. In addition, we would like to study the intracellular localization of processed HCV proteins, as well as virus assembly and the effects of specific antibodies and inhibitors. All of these things need to be done. Nevertheless, the evidence of infectivity of HCV RNA shown in the present work illustrates the potential of reverse genetics to delineate the mechanism

of HCV replication at a molecular level. This system will no doubt prove quite useful for studying the mechanism of persistent HCV infection and to evaluate the efficacy of vaccines, as well as various HCV specific inhibitors.

Materials and methods

Inoculum

We used plasma (no. 6) from a donor known to carry infectious HCV. Competitive RT-PCR detected 10^5 genome/ml of HCV RNA in the plasma (Sugitani and Shikata, 1998). pCV-H77C, which contains a full-length cDNA clone of strain H77 of HCV, was kindly provided by Dr. J. Bukh, National Institutes of Health, USA (Yanagi et al., 1997). We also constructed two full-length mutant clones (H77cHel- and H77cRdRp-) of HCV, containing D1316A (4286 to 4289), and G2737A (8551 to 8552), D2738A (8554), and D2739G (8557 to 8559) substitutions, respectively (Kolykhalov et al., 2000).

RFB culture of FLC4 cells

We developed a RFB culture system (Able, Japan) (Kawada et al., 1998; Matsuura et al., 1998) of FLC4 cells, produced from the cloning of JHH4 cells, in an attempt to maintain hepatocyte function in culture for an extended period of time. The RFB system, having an area of 2.7 m^2, was seeded with 1×10^9 FLC4 cells. Culture medium containing 2% FCS was added at a flow rate of 50 ml/day. To monitor the viability of cells, oxygen and glucose consumption, as well as albumin secretion, were continuously monitored throughout the duration of the study. The culture temperature was reduced from 37 to 35°C immediately following inoculation with plasma, and again to 32°C on day 51 p.i. to maintain continual slow growth of cells. As a consequence, oxygen consumption increased steadily, reaching 250 mg/day by day 30 p.i. and 350 mg/day by day 70 p.i. Despite the effects of low temperature on the culture, albumin secretion remained above 75 μg/ml throughout the culture period of 100 days.

Infection and transfection

In the infection experiments, FLC4 cells were seeded in the RFB and cultured in ASF medium (Ajinomoto, Tokyo, Japan), containing 2% fetal calf serum, at a flow rate of 100 ml/day. One milliliter of plasma no. 6 was added, after which HCV RNA and ALT levels were measured in the culture fluid. To maintain an oxygen concentration of less than 1.0 ppm at the RFB outlet during culture, the culture temperature was gradually reduced from 37 to 32°C.

In the transfection experiments, serum-free ASF medium was added to FLC4 cells in RFB culture at a rate of 50 ml/day. pCV-H77C, pCV-H77cHel-, or pCV-H77cHel- was linealized with *Xba*I, and 10 μg of each RNA transcript was mixed with lipofectin (Invitrogen, Carlsbad, CA) and diluted with 10 ml of Opti-MEM (Invitrogen). The mixture was then used to inoculate cells in the RFB.

For secondary passage, supernatant was collected on days 93, 94, and 95 p.t. (pooled to approximately 150 ml) and frozen at −80°C, until which time it was thawed and centrifuged at 8000 *g* for 15 min. After this, the supernatant, containing approximately 1.5×10^6 copies of HCV, was transferred to new FLC4 cells in RFB culture. Fifty milliliters of culture fluid was collected every day and replaced with 50 ml of new, fresh medium.

Analysis and quantitation of HCV RNA

HCV RNA in the medium was qualitatively detected by RT-PCR as described previously (Aizaki et al., 1998). Quantitative determination of HCV RNA was performed according to the competitive PCR method described by Kaneko et al. (1992). The limit of detection for HCV RNA by quantitative PCR was 10^3 copies/ml (Aizaki et al., 1998). RT-PCR was performed independently in two different laboratories (National Institute of Infectious Diseases and Mitsubishi Kagaku Bio-clinical Laboratories, Japan), and the same results were obtained. The nucleotide and amino acid sequences of HVRs of HCV envelope glycoprotein E2 were compared. Treatment with RNase was done as described previously by Kolykhalov et al. (1997). Negative-stranded HCV RNA was detected by strand-specific PCR as described previously by Lanford et al. (1994). Synthetic positive-and negative-strand RNAs encompassing the 5′ untranslated region of HCV were prepared by in vitro transcription using T7 RNA polymerase, followed by extensive purification with DNase to remove DNA. The purified RNAs were mixed with cellular RNA from FLC4 to mimic the conditions of transfected cells and to check for the generation of false positives by PCR. PCR products from one round of amplification were analyzed by agarose gel electrophoresis.

Enzyme immunoassay for HCV core antigen

The culture medium was centrifuged at 8000 *g* for 90 min, after which the supernatant was centrifuged at 100,000 *g* for 3 h. The precipitates were suspended in lysis buffer (Promega, Madison, WI) and HCV core antigen was measured using the highly sensitive enzyme immunoassay (EIA) method (Kashiwakuma et al., 1996).

Electron microscopy study

Cell samples for TEM and SEM were prepared as described previously (Kawada et al., 1998). Briefly, FLC4 cells in RFB culture were fixed in 2.5% glutaraldehyde in 0.1 M phosphate buffer (pH 7.4). After treatment with 0.1% osmium tetroxide in the same buffer, specimens were de-

hydrated in ethanol, after which they were embedded in a mixture of propyloxide and EPOK812 epoxy resin. Thin sections were examined with a transmission electron microscope (JEOL DEM1200-EX, Nihon Denshi Co., Japan). FLC4 cells attached to microcarriers were fixed to the observation table and dehydrated, after which they were submerged in 100% isoamine acetate. Samples coated with carbon and gold were observed with a scanning electron microscope (JEOL-35CF, Nihon Denshi Co.).

To analyze the virus-like particles, culture fluid of cells transfected with HCV RNA was collected and concentrated by ultracentrifugation. The pellet obtained by centrifugation was suspended in 1.5 ml of ASF medium and one-third of the suspension was reconcentrated. After this, the resultant pellet was suspended in 3 μl of ASF medium and applied to a formvar-carbon grid for negative staining. For IEM study, mouse monoclonal antibody against HCV E1 protein (1:10 dilution) and goat anti-mouse IgG-conjugated colloidal gold particles (6 nm; 1:20 dilution) were used as first and second antibodies, respectively.

Acknowledgments

We thank Drs. J. Bukh and R. Purcell for providing a full-length HCV cDNA. This work was supported by Grants-in-Aid from the Second-Term Comprehensive 10-Year Strategy for Cancer Control, Research on Advanced Medical Technology, Research on Emerging and Re-emerging Infectious Diseases from the Ministry of Health and Welfare, the Organization for Pharmaceutical Safety and Research, Japan, and the Promotion and Mutual Aid Corporation for Private Schools of Japan.

References

Aizaki, H., Aoki, Y., Harada, T., Ishii, K., Suzuki, T., Nagamori, S., Toda, G., Matsuura, Y., Miyamura, T., 1998. Full-length complementary DNA of hepatitis C virus genome from an infectious blood sample. Hepatology 27, 621–627.

Aoki, Y., Aizaki, H., Shimoike, T., Tani, H., Ishii, K., Saito, I., Matsuura, Y., Miyamura, T., 1998. A human liver cell line exhibits efficient translation of HCV RNAs produced by a recombinant adenovirus expressing T7 RNA polymerase. Virology 250, 140–150.

Bartenschlager, R., Lohmann, V., 2001. Novel cell culture systems for the hepatitis C virus. Antiviral Res. 52, 1–17.

Blight, K.J., Kolykhalov, A.A., Rice, C.M., 2000. Efficient initiation of HCV RNA replication in cell culture. Science 290, 1972–1974.

Boulan, E.R., Sabatini, D.D., 1978. Asymmetric budding of viruses in epithelial monolayers: a model system for study of epithelial polarity. Proc. Natl. Acad. Sci. USA 75, 5071–5075.

Boyer, J.C., Haenni, A.L., 1994. Infectious transcripts and cDNA clones of RNA viruses. Virology 198, 415–426.

Choo, Q.-L., Kuo, G., Weiner, A.J., Overby, L.R., Bradley, D.W., Houghton, M., 1989. Isolation of a cDNA clone derived from a blood-borne non-A, non-B viral hepatitis genome. Science 244, 359–362.

Ikeda, M., Yi, M.-K., Li, K., Lemon, S.M., 2002. Selectable subgenomic and genome-length dicistronic RNAs derived from an infectious molecular clone of the HCV-N strain of hepatitis C virus replicate efficiently in cultured Huh7 cells. J. Virol. 76, 2997–3006.

Ilan, E., Arazi, J., Nussbaum, O., Zauberman, A., Eren, R., Lubin, I., Neville, L., Ben-Moshe, O., Kischitzky, A., Litchi, A., Margalit, I., Gopher, J., Mounir, S., Cai, W., Daudi, N., Eid, A., Jurim, O., Czerniak, A., Galun, E., Dagan, S., 2002. The hepatitis C virus (HCV)-trimera mouse: a model for evaluation of agents against HCV. J. Infect. Dis. 185, 153–161.

Ito, T., Yasui, K., Mukaigawa, J., Katsume, A., Kohara, M., Mitamura, K., 2001. Acquisition of susceptibility to hepatitis C virus replication in HepG2 cells by fusion with primary human hepatocytes: establishment of a quantitative assay for hepatitis C virus infectivity in a cell culture system. Hepatology 34, 566–72.

Kaito, M., Wastanabe, S., Tsukiyama-Kohara, K., Yamaguchi, K., Kobayashi, Y., Konishi, M., Yokoi, M., Ishida, S., Suzuki, S., Kohara, M., 1994. Hepatitis C virus particle detected by immunoelectron microscopic study. J. Gen. Virol. 75, 1755–1760.

Kaneko, S., Murakami, S., Unoura, M., Kobayashi, K., 1992. Quantitation of hepatitis C virus RNA by competitive polymerase chain reaction. J. Med. Virol. 37, 278–282.

Kanto, T., Hayashi, N., Takehara, T., Hagiwara, H., Mita, E., Naito, M., Kasahara, A., Fusamoto, H., Kamada, T., 1994. Buoyant density of hepatitis C virus recovered from infected hosts: two different features in sucrose equilibrium density-gradient centrifugation related to degree of liver inflammation. Hepatology 19, 296–302.

Kashiwakuma, T., Hasegawa, A., Kajita, T., Takata, A., Mori, H., Ohta, Y., Tanaka, E., Kiyosawa, K., Tanaka, T., Tanaka, S., Hattori, N., Kohara, M., 1996. Detection of hepatitis C virus specific core protein in serum of patients by a sensitive fluorescence enzyme immunoassay (FEIA). J. Immunol. Methods 190, 79–89.

Kato, N., Shimotohno, K., 1999. Systems to culture hepatitis C virus, in: Hagedorn, C.H., Rice, C.M. (Eds.), The Hepatitis C Viruses, Springer, Berlin, pp. 261–278.

Kawada, M., Nagamori, S., Aizaki, H., Fukaya, K., Niiya, M., Matsuura, T., Sujino, H., Hasumura, S., Yashida, H., Mizutani, S., Ikenaga, H., 1998. Massive culture of human liver cancer cells in a newly developed radial flow bioreactor system: ultrafine structure of functionally enhanced hepatocarcinoma cell lines. In Vitro Cell. Dev. Biol. Anim. 34, 109–115.

Koike, K., Tsutsumi, T., Fujie, H., Shintani, Y., Kyoji, M., 2002. Molecular mechanism of viral hepatocarcinogenesis. Oncology 62, 29–37.

Kolykhalov, A.A., Agapov, E.V., Blight, K.J., Mihalik, K., Feinstone, S.M., Rice, C.M., 1997. Transmission of hepatitis C by intrahepatic inoculation with transcibed RNA. Science 277, 570–574.

Kolykhalov, A.A., Mihalik, K., Feinstone, S.M., Rice, C.M., 2000. Hepatitis C virus-encoded enzymatic activities and conserved RNA elements in the 3′ nontranslated region are essential for virus replication in vivo. J. Virol. 74, 2046–2051.

Krieger, N., Lohmann, V., Bartenschlager, R., 2001. Enhancement of hepatitis C virus RNA replication by cell culture-adaptive mutations. J. Virol. 75, 4614–4624.

Kuo, G., Choo, Q.-L., Alter, H.J., Gitnick, G.L., Redeker, A.G., Purcell, R.H., Miyamura, T., Dienstag, J.L., Alter, M.J., Stevens, C.E., Tegtmeier, G.E., Bonino, F., Colombo, M., Lee, W.-S., Kuo, C., Berger, K., Shuster, F.R., Overby, L.R., Bradley, D.W., Houghton, M., 1989. An assay for circulating antibodies to a major etiologic virus of human non-A, non-B hepatitis. Science 244, 362–364.

Lanford, R.E., Sureau, C., Jacob, J.R., White, R., Fuerst, T.R., 1994. Demonstration of in vitro infection of chimpanzee hepatocytes with hepatitis C virus using strand-specific RT/PCR. Virology 202, 606–614.

Lohmann, V., Komer, F., Dobierzewska, A., Bartenschlager, R., 2001. Mutations in hepatitis C virus RNAs conferring cell culture adaptation. J. Virol. 75, 1437–1449.

Lohmann, V., Komer, F., Koch, J., Herian, U., Theilmann, L., Bartenschlager, R., 1999. Replication of subgenomic hepatitis C virus RNAs in a hepatoma cell line. Science 285, 110–113.

Matsuura, T., Kawada, M., Hasumura, S., Nagamori, S., Obata, T., Yamaguchi, M., Hataba, Y., Tanaka, H., Shimizu, H., Unemura, Y., Nonaka, K., Iwaki, T., Kojima, S., Aizaki, H., Mizutani, S., Ikenaga, H., 1998. High density culture of immortalized liver endothelial cells in the radial-flow bioreactor in the development of an artificial liver. Int. J. Artif. Organs 21, 229–234.

Mercer, D.F., Schiller, D.E., Elliott, J., Douglas, D.N., Hao, C., Rinfret, A., Addison, W.R., Fischer, K.P., Churchill, T.A., Lakey, J.R.T., Tyrrell, D.L.J., Kneteman, N.M., 2001. Hepatitis C virus replication in mice with chimeric human livers. Nat. Med. 7, 927–933.

Pietschmann, T., Lohmann, V., Kaul, A., Krieger, N., Rinck, G., Rutter, C., Strand, D., Bartenschlager, R., 2002. Persistent and transient replication of full-length hepatitis C virus genomes in cell culture. J. Virol. 76, 4008–4021.

Randall, G., Rice, C.M., 2001. Hepatitis C virus cell culture replication systems: their potential use for the development of antiviral therapies. Curr. Opin. Infect. Dis. 14, 743–747.

Saito, I., Miyamura, T., Ohbayashi, A., Harada, H., Katayama, T., Kikuchi, S., Watanabe, Y., Koi, S., Onji, M., Ohta, Y., Choo, Q.-L., Houghton, M., Kuo, G., 1990. Hepatitis C virus infection is associated with the development of hepatocellular carcinoma. Proc. Natl. Acad. Sci. USA 87, 6547–6549.

Sugitani, M., Shikata, T., 1998. Comparison of amino acid sequences in hypervariable region-1 of hepatitis C virus clones between human inocula and the infected chimpanzee sera. Virus Res. 56, 177–182.

Takeuchi, K., Boonmar, S., Kubo, Y., Katayama, T., Harada, H., Ohbayashi, A., Choo, Q.-L., Kuo, G., Houghton, M., Saito, I., Miyamura, T., 1990. Hepatitis C virus cDNA clones isolated from a healthy carrier donor implicated in post-transfusion non-A, non-B hepatitis. Gene 91, 287–291.

Takikawa, S., Ishii, K., Aizaki, H., Suzuki, T., Asakura, H., Matsuura, Y., Miyamura, T., 2000. Cell fusion activity of hepatitis C virus envelope proteins. J. Virol. 74, 5066–5074.

Thomson, M., Liang, T.J., 2000. Molecular biology of hepatitis C virus, in: Liang, T.J., Hoofnagle, J.H. (Eds.), Hepatitis C. Academic Press, San Diego, pp. 1–24.

Yanagi, M., Purcell, R.H., Emerson, S.U., Bukh, J., 1997. Transcripts from a single full-length cDNA clone of hepatitis C virus are infectious when directly transfected into the liver of a chimpanzee. Proc. Natl. Acad. Sci. USA 94, 8738–8743.

Hepatitis C Virus Core Protein Activates ERK and p38 MAPK in Cooperation With Ethanol in Transgenic Mice

Takeya Tsutsumi,[1,2] Tetsuro Suzuki,[1] Kyoji Moriya,[2] Yoshizumi Shintani,[2] Hajime Fujie,[2] Hideyuki Miyoshi,[2] Yoshiharu Matsuura,[3] Kazuhiko Koike,[2] and Tatsuo Miyamura[1]

In human chronic hepatitis C, alcohol intake is a synergistic factor for the acceleration of hepatocarcinogenesis. Recently, we showed a significant increase of reactive oxygen species (ROS) in hepatitis C virus (HCV) core-transgenic mice fed ethanol-containing diets. Because previous studies indicated that ROS is closely associated with mitogen-activated protein kinases (MAPK), we examined activities of c-Jun N-terminal kinase, p38 MAPK, and extracellular signal-regulated kinase (ERK) in the liver of core-transgenic and nontransgenic mice with short-term ethanol feeding. Activity of ERK and p38 MAPK was increased in core-transgenic mice compared with nontransgenic mice, whereas neither ERK nor p38 MAPK was activated in core-transgenic mice with normal diets. In addition, activity of cyclic-AMP and serum responsive element, downstream pathways of p38 MAPK and ERK, was also increased. Comparison of gene expression profiles by cDNA microarray and real-time PCR revealed that galectin-1, which is associated with cell transformation, was significantly increased in ethanol-fed core-transgenic mice. On the other hand, glutathione S-transferase (GST), which plays a key role in protecting cells from oxidative stress, was decreased. In conclusion, these results suggest that HCV core protein cooperates with ethanol for the activation of some MAPK pathways, and leads to the modulation of several genes, contributing to the pathogenesis of liver disease of HCV-infected patients with high ethanol consumption. (HEPATOLOGY 2003;38:820-828.)

Chronic hepatitis C virus (HCV) infection is associated with the development of hepatocellular carcinoma (HCC).[1] The precise mechanism of hepatocarcinogenesis in HCV infection is, however, not yet clearly elucidated. Inflammation definitely plays important roles.[2,3] However, the fact that chronic hepatitis by HCV, but not autoimmune or alcoholic hepatitis, is frequently accompanied by the HCC development suggests that HCV proteins also play direct roles in hepatocarcinogenesis. Among HCV viral proteins, the core protein is intensively investigated for its functions to modulate cellular processes such as apoptosis, cell proliferation, and transformation.[4] In addition, we showed that transgenic mice expressing the core protein develop HCC later in their lives without coexisting inflammation.[5] These findings suggest that the core protein is one of the main factors responsible for the HCC development in HCV infection. Further examination of core-transgenic mice suggested that the core protein expression in the liver induces oxidative stress and that host cells in turn protect themselves by modulating the defense system to keep the intracellular redox balance.[6] However, ethanol feeding for 3 weeks in the core-transgenic mice disrupted this balance, leading to enhanced intracellular reactive oxygen species (ROS) generation and, possibly, DNA damage.[6] This is of great interest because excessive alcohol intake has been documented as an independent cofactor accelerating the HCC development in chronic hepatitis C patients.[7-9] In view of these findings, our core-transgenic

Abbreviations: HCV, hepatitis C virus; HCC, hepatocellular carcinoma; ROS, reactive oxygen species; MAPK, mitogen-activated protein kinase; ERK, extracellular signal-regulated kinase; JNK, c-Jun N-terminal kinase; IKK, IκB kinase; NF-κB, nuclear factor-κB; SDS, sodium dodecyl sulfate; GST, glutathione S-transferase; GAPDH, glyceraldehyde 3-phosphate dehydrogenase; EMSA, electrophoretic mobility shift assay; CRE, cyclic AMP responsive element; SRE, serum responsive element; ATF-2, anti-activating transcription factor-2; RT-PCR, reverse-transcription polymerase chain reaction.

From the [1]Department of Virology II, National Institute of Infectious Diseases, Tokyo; [2]Department of Internal Medicine, Faculty of Medicine, University of Tokyo, Tokyo; and [3]Research Center for Emerging Infectious Diseases, Research Institute for Microbial Diseases, Osaka University, Osaka, Japan.

Received March 4, 2003; accepted July 1, 2003.

Supported in part by Second Term Comprehensive 10-Year Strategy for Cancer Control; Health Sciences Research Grants of The Ministry of Health and Welfare; grants from The Ministry of Education, Science, and Culture of Japan; and by the program for Promotion of Fundamental Studies in Health Sciences of the Organization for Drug ADR Relief, R&D Promotion, and Product Review of Japan.

T.T. is a research fellow of The Organization for Pharmaceutical Safety and Research.

Address reprint requests to: Tatsuo Miyamura, M.D., Department of Virology II, National Institute of Infectious Diseases, 1-23-1, Toyama, Shinjuku-ku, Tokyo 162-8640, Japan. E-mail: tmiyam@nih.go.jp; fax: (81) 3-5285-1161.

0270-9139/03/3804-0007$30.00/0

doi:10.1053/jhep.2003.50399

mouse is a suitable model for investigating the molecular event occurring in human livers with HCV infection and ethanol loading.

Mitogen-activated protein kinases (MAPKs) are a family of serine/threonine kinases involved in the regulation of a wide range of cellular responses, including cell proliferation, differentiation, stress adaptation, and apoptosis.[10] Based on structural differences, they are divided into 3 multimer subfamilies: extracellular signal-regulated kinase (ERK), c-Jun N-terminal kinase (JNK), and p38 MAPK. The ERK, JNK, and p38 MAPK are activated via dependent signaling cascades involving a MAPK kinase that is responsible for phosphorylation of the MAPK. MAPKs mediate their effects through phosphorylation of effector proteins, notably transcription factors, which in turn lead to changes in the pattern of gene expression. It is known that MAPKs are activated by a number of growth factors and cytokines via their specific receptors expressed on the cell surface.[10] Besides these extracellular stimuli, the association of intracellular ROS with MAPK activation has been reported.[11-14] A low level oxidative stress, which lacks apoptosis induction, causes selective activation of p38 MAPK cascade and mitotic arrest in human lymphoid cells.[11] Another study showed that increased ERK and p38 MAPK activities are important components of ROS-mediated signaling in mouse keratinocytes.[12] Also in hepatocytes, several studies showed that oxidative stress induces the activation of p38 MAPK and ERK.[13,14]

In the present study, we investigated the activation of MAPK signaling pathways, ERK, p38 MAPK, and JNK as well as IκB kinase (IKK)–nuclear factor-κB (NF-κB) in the liver of core-transgenic mice fed with short-term, ethanol-containing diets. We found that ERK and p38 MAPK and their downstream transcription factors were activated in these mice but that JNK and IKK–NF-κB were not. We further examined genes of differential expression in the liver of ethanol-fed core-transgenic mice and found that expression of several genes related to cellular processes such as cell proliferation and antioxidants was modulated.

Materials and Methods

Transgenic Mice. Production of HCV core gene (genotype Ib) transgenic mice (C57BL/6) was previously described.[15] For the ethanol-loading experiment, mice were fed diets containing 5% ethanol (Oriental Yeast Co., Tokyo, Japan) for 3 weeks.[6] Pairs of male, transgenic and nontransgenic mice from 3 to 6 months of age were used. These mice had almost normal livers or very mild steatosis, if any, whereas nontransgenic mice had normal livers. Neither inflammatory changes nor tumorous lesions in the liver were observed in any of these mice.

Western Blotting. Liver tissues of mice were lysed in RIPA buffer (10 mmol/L Tris-HCl [pH 7.4], 150 mmol/L NaCl, 1% sodium deoxycholate, 0.1% sodium dodecyl sulfate (SDS), and 1% Triton-X 100) containing Protease Inhibitor Cocktail (Complete; Roche Molecular Biochemicals, Indianapolis, IN). Western blotting was performed as described previously.[16] For the detection of ERK1/2, phosphorylated ERK1/2, galectin-1, metallothionein, glutathione S-transferase (GST)-pi, p27Kip1, and glyceraldehyde 3-phosphate dehydrogenase (GAPDH), the membrane was probed with anti-ERK1/2 (Cell Signaling Technology, Beverly, MA), anti-phospho-ERK1/2 (Cell Signaling), anti-galectin-1 (Novocastra Laboratories, Newcastle, United Kingdom), anti-metallothionein (StressGen Biotechnologies, Victoria, Canada), anti-GST-pi (NeoMarkers, Fremont, CA), anti-p27Kip1 (Cell Signaling), and anti-GAPDH (Chemicon International, Temecula, CA), respectively.

In Vitro *Kinase Assay.* Samples for the kinase assay were prepared as described previously.[16] Activities of JNK, p38 MAPK, and ERK1/2 were determined using SAPK/JNK Assay Kit, p38 MAP Kinase Assay Kit, and p44/42 MAP Kinase Assay Kit (Cell Signaling), respectively. MAPK activity was determined by measuring the intensity of the band by densitometer (NIH Image; National Institutes of Health, Bethesda, MD). Activity of IKK was determined as described previously.[16]

Electrophoretic Mobility Shift Assay. Electrophoretic mobility shift assay (EMSA) was performed as described previously.[16] The oligonucleotides used were as follows: 5′-AGA GAT TGC CTG ACG TCA GAG AGC TAG-3′ for cyclic AMP responsive element (CRE), 5′-GGA TGT CCA TAT TAG GAC ATC-3′ for serum responsive element (SRE), and 5′-AGT TGA GGG GAC TTT CCC AGG C-3′ for NF-κB–binding element. The binding buffer for CRE assay was composed of 20 mmol/L Tris-HCl (pH 7.4), 10 mmol/L NaCl, 1 mmol/L EDTA, 12% glycerol, 1.7 mmol/L dithiothreitol, 0.7% bovine serum albumin, and 2 μg of poly (dI-dC). For SRE assay, 5 mmol/L $MgCl_2$ was added to the binding buffer for NF-κB.[16] For super shift experiment, 1 μg of antiactivating transcription factor-2 (ATF-2) antibody (Santa-Cruz Biotechnology, Santa Cruz, CA) was added and incubated at room temperature for 30 minutes.

Microarray Analysis. The GeneNavigator cDNA Array System-Mouse Cancer (Toyobo, Osaka, Japan) was used for the analysis. Four hundred thirty-four species of mouse DNA fragments are spotted in duplicate on the

filter. The genes include cancer-related genes, housekeeping genes, and nonmammalian genes as negative controls. mRNA was isolated by incubation with oligo-dT-magnetic beads (Toyobo). The probes were constructed using reverse transcription, labelled with biotin. The filters were preincubated in PerfectHyb (Toyobo) for 30 minutes, then hybridized with denatured probes at 68°C overnight. After washing, specific signals were detected by Imaging High Chemifluoresecence Detection Kit (Toyobo). The signal intensity among filters was compared by E-Gene Navigator Analysis (GeneticLab, Sapporo, Japan). Intensity that was twice as high as the background was defined as a positive signal. The intensity of each spot was corrected by subtracting the background signals and normalized using that of GAPDH. Genes that were 1.25-fold increased or decreased in both of the 2 core-transgenic mice were defined as up-regulated or down-regulated, respectively.

Real-Time Reverse-Transcription Polymerase Chain Reaction. TaqMan real-time reverse-transcription polymerase chain reaction (RT-PCR) was performed as described previously, using ABI Prism 7700 Sequence Detector (Applied Biosystems, Foster City, CA).[16] Primers and the TaqMan probes for galectin-1, GST-P1, and p27Kip1 were as follows: galectin-1 forward primer: 5′-GCTGCCAGACGGACATGAA-3′, reverse primer: 5′-CATCCGCCGCCATGTAGT-3′, probe: 5′-AGTTCCCAAACCGCCTCAACATGGA-3′; GST-P1 forward primer: 5′-CATCGTGGGTGACCAGATCTC-3′, reverse primer: 5′-GCCAGGACTTGGTGGATCAG-3′, probe: 5′-TGCCGATTACAACTTGCTGGACCTGC-3′; p27Kip1 forward primer: 5′-GGTGGACCAAATGCCTGACT-3′, reverse primer: 5′-CAGCAGGTCGCTTCCTCATC-3′, probe: 5′-TCCGCTAACCCAGCCTGATTGTCTGA-3′.

Statistical Analysis. Results are expressed as means ± SE. The significance of the difference of means was determined using the Mann-Whitney *U* test.

Results

Activation of p38 MAPK and ERK in the Liver of the Transgenic Mice Fed With Ethanol. We first investigated the effect of ethanol feeding on MAPK activity in the liver of core-transgenic mice. Activities of ERK, p38 MAPK, and JNK were determined by *in vitro* kinase assay. Interestingly, activities of ERK and p38 MAPK were increased in the liver of core-transgenic mice fed with 5% ethanol-containing diets (Fig. 1A). Densitomery showed that ERK and p38 MAPK were 2-fold and 2.5-fold activated, respectively (Fig. 1B). We also examined mice with normal diets and found that activitation of these MAPKs was similar between core-transgenic and nontransgenic mice (Fig. 1A and B). These results indicated that the core protein and ethanol cooperatively work for the activation of p38 MAPK and ERK. On the other hand, JNK activity, which was increased in normal-diet core-transgenic mice,[16] was similar between ethanol-fed core-transgenic, and nontransgenic mice (Fig. 1A and B).

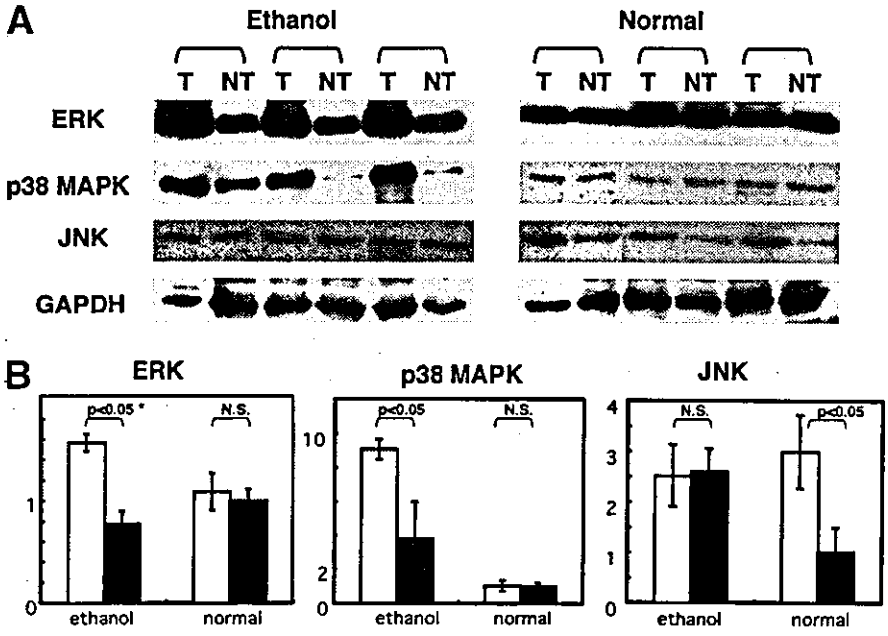

Fig. 1. Activity of MAPK in the liver of core-transgenic mice. (A) Activity of ERK, p38 MAPK, and JNK in the liver of core-transgenic (T) and nontransgenic (NT) mice was determined by *in vitro* kinase assay according to the protocols shown in the Materials and Methods section. Western blotting of GAPDH using 10 μg of the same cell lysates was shown in the lowest panels. (B) The intensity of the bands shown in (A) is normalized by that of GAPDH and analyzed by densitometry. **Open** and **solid columns** indicate core-transgenic and nontransgenic mice, respectively. Values are normalized by taking the intensity of normal-diet nontransgenic mice as 1 (relative kinase activity). Data shown are means ± SE. *Mann-Whitney *U* test. NS, not statistically significant.

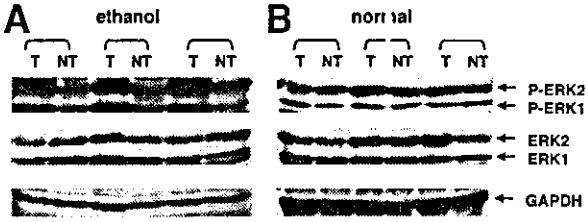

Fig. 2. Protein levels of phosphorylated ERK (P-ERK) in the liver of core-transgenic mice. Tissue lysates of the liver of core-transgenic (T) and nontransgenic (NT) mice were separated on a 10% SDS-PAGE gel and immunoblotted for phosphorylated forms of ERK **(upper panels)**, whole ERK **(middle panels)**, and GAPDH **(lower panels)**. (A) Mice fed with ethanol-containing diets. (B) Mice fed with normal diets. ERK1 and ERK2 correspond to 42- and 44-kd form of ERK, respectively.

Activation of ERK results from phosphorylation of threonine and tyrosine at the sequence Thr*-Glu-Tyr* by an upstream MAPK kinase.[17] We therefore determined the phosphorylation levels of ERK using an antibody that specifically detects phosphorylated ERK. Levels of phosphorylated ERK were increased in ethanol-fed core-transgenic mice compared with nontransgenic mice (Fig. 2A), whereas similar levels of phosphorylated ERK were observed between core-transgenic and nontransgenic mice with normal diets (Fig. 2B). This result further confirms that ERK was activated through phosphorylation in ethanol-fed core-transgenic mice.

Activation of Downstream Transcription Factors. ERK and p38 MAPK are known to activate several transcription factors. Among them, ATF-2 is phosphorylated and activated by p38 MAPK leading to bind to the DNA motif called *CRE*.[18] Therefore, we next determined the activation of ATF-2. As shown in Fig. 3A, proteins bound to CRE were increased in the liver of ethanol-fed core-transgenic mice. Super shift analysis suggested that this shifted band was mainly composed of ATF-2/DNA complex (Fig. 3A, lanes 8 and 9). Because Elk-1, which binds to SRE, was activated mainly by ERK,[19] we also determined SRE activation. As shown in Fig. 3B, activity of SRE was increased in ethanol-fed core-transgenic mice. However, in normal-diet, core-transgenic and nontransgenic mice, no shifted bands were seen. This is probably due to the low activation of SRE, which is below the detection limit of this experimental system. We confirmed activation of CRE and SRE also in other ethanol-fed core-transgenic mice (data not shown). These results indicated that CRE and SRE, downstream effectors of p38 MAPK and ERK, are also activated in core-transgenic mice with ethanol-containing diets.

Activation of IKK–NF-κB Pathway. We recently reported that intrahepatic expression levels of tumor necrosis factor α and interleukin 1β (IL-1β) in core-transgenic mice were increased, while one of their downstream pathways, IKK–NF-κB, was not activated.[16] Therefore, we next examined whether IKK–NF-κB pathway was activated with ethanol-containing diets. We first determined IKK activity by *in vitro* kinase assay using GST–IκB-α as a substrate. As shown in Fig. 4A, IKK activity was similar between core-transgenic and nontransgenic mice, regardless of ethanol in diets. IKK activity in ethanol-fed mice was about 1.5-fold increased compared with normal-diet mice (Fig. 4B), indicating that ethanol feeding itself has some effects on IKK activation. We next investigated NF-κB activation in these mice by EMSA. As expected from IKK activity, NF-κB was similarly activated in ethanol-fed mice, but there were no differences between core-transgenic and nontransgenic mice (Fig. 4C). These results suggest that the core protein has no effects on the IKK–NF-κB pathway even in the presence of ethanol in core-transgenic mice.

Identification of Transcriptionally Modulated Genes. Activation of p38 MAPK-CRE and ERK-SRE pathways encouraged us to investigate genes differentially expressed in the liver of ethanol-fed core-transgenic mice. We performed microarray analysis to identify differentially expressed genes related to cellular processes such as apoptosis and cell cycle. We examined 2 pairs of ethanol-fed core-transgenic and nontransgenic mice and compared expression levels in the 2 core-transgenic mice with the average levels in 2 nontransgenic mice. The intensity

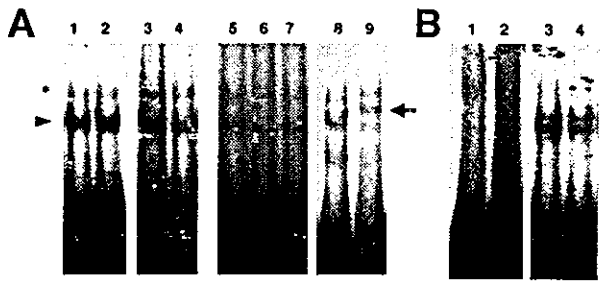

Fig. 3. Activity of transcription factors in the liver of core-transgenic mice. Nuclear proteins extracted from the liver of mice were incubated with ^{32}P-labeled oligonucleotides containing corresponding consensus sequence then loaded onto nondenaturing gels. (A) CRE activity. **Lane 1**, normal-diet core-transgenic mouse; **lane 2**, normal-diet nontransgenic mouse; **lane 3**, ethanol-fed core-transgenic mouse; **lane 4**, ethanol-fed nontransgenic mouse; **lanes 5-7**, competition assay; **lane 5**, no nonlabeled oligonucleotides; **lane 6**, addition of 50-fold of nonlabeled CRE binding consensus oligonucleotides; **lane 7**, addition of 50-fold of nonlabeled NF-κB binding consensus oligonucleotides; **lanes 8 and 9**, super shift assay; **lane 8**, no antibody; **lane 9**, preincubation with anti-ATF-2 antibody. **Arrowhead** and **arrow** indicate DNA-ATF2 and DNA-ATF2-antibody complexes, respectively. An **asterisk** is a nonspecific band. (B) SRE activity. **Lane 1**, normal-diet core-transgenic mouse; **lane 2**, normal-diet nontransgenic mouse; **lane 3**, ethanol-fed core-transgenic mouse; **lane 4**, ethanol-fed nontransgenic mouse. **Arrowhead** indicates SRE-binding protein.

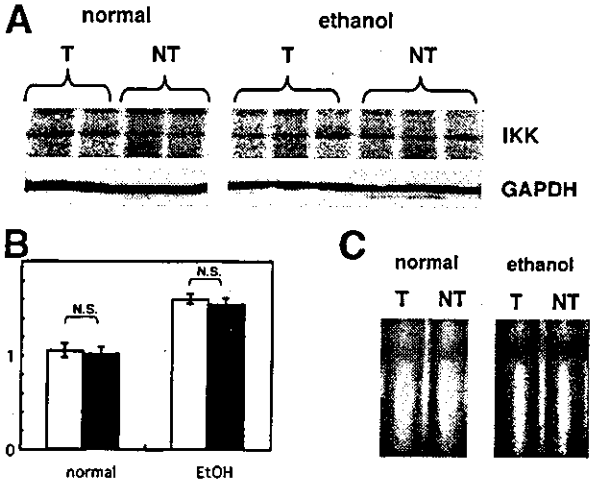

Fig. 4. Activity of IKK and NF-κB in the liver of core-transgenic (T) and nontransgenic (NT) mice. (A) Activity of IKK determined by *in vitro* kinase assay. IKK was immunoprecipitated by anti-IKK antibody from lysates of mouse liver and incubated with GST-IκB-α in the presence of [γ-^{32}P]ATP. Western blotting of GAPDH using the same cell lysates was shown in **lower panels**. (B) Densitometry analysis of the blots shown in (A). IKK activity was determined by dividing the intensity of phosphorylated GST-IκB-α by that of GAPDH. **White** and **black columns** indicate core-transgenic and nontransgenic mice, respectively. Values are normalized by taking the average intensity of normal-diet nontransgenic mice as 1 (relative kinase activity). Data shown are means ± SE. NS, not statistically significant (Mann-Whitney *U* test). (C) NF-κB activation determined by EMSA. **Lane 1**, normal-diet core-transgenic mouse; **lane 2**, normal-diet nontransgenic mouse; **lane 3**, ethanol-fed core-transgenic mouse; **lane 4**, ethanol-fed nontransgenic mouse.

of signals in each spot was similar in 2 nontransgenic mice (data not shown). We selected genes whose expression levels were 1.25-fold changed. Two genes were up-regulated, and 6 genes were down-regulated in the liver of ethanol-fed core-transgenic mice (Table 1). Notably, several antioxidant-related genes such as GST and metallothionein were included in these down-regulated genes, which may be associated with ROS generation in ethanol-fed core-transgenic mice. In addition, galectin-1, shown to be associated with cell transformation by interaction with Ras, was most up-regulated.[20] In several genes whose promoter region contains CRE or SRE, the intensity of signals was also increased in core-transgenic mice. They were proliferating cell nuclear antigen, CRE-binding protein, IL-6, and matrix metalloprotease-9.[21,22] However, the intensity in these genes was so weak that we could not include them in Table 1 according to the criteria described in the Materials and Methods section.

mRNA Expression Levels of Differentially Regulated Genes. We next determined mRNA expression levels of differentially expressed genes. To this aim, we quantified mRNA levels of genes of interest as well as GAPDH by using the real-time TaqMan RT-PCR method and calculated the relative amount by dividing the amount of target genes by that of GAPDH gene. Among up-regulated genes, we first focused on galectin-1, whose expression levels were the most increased in both of the 2 core-transgenic mice. As shown in Table 2, galectin-1 gene expression was significantly (8-fold) enhanced in ethanol-fed core-transgenic mice. In normal-diet core-transgenic mice, levels of galectin-1 gene expression were higher, although not significantly, than those in nontransgenic mice. In core-transgenic mice, expression of galectin-1 was about 3-fold increased by ethanol, whereas almost no increase could be seen in nontransgenic mice. These results suggest that the core protein accelerated expression of galectin-1 gene and that this acceleration was further enhanced by ethanol feeding.

We then determined mRNA expression levels of GST-P1 (one of the down-regulated genes) and p27Kip1 (one of the up-regulated genes). As shown in Table 2, levels of GST-P1 expression were significantly decreased in ethanol-fed core-transgenic mice. In contrast to the galectin-1 gene, however, GSTP1 gene expression was not significantly different between core-transgenic and

Table 1. Differentially Expressed Genes in the Liver of Ethanol-Fed Core-Transgenic Mice

Gene	Fold Change (T1)	Fold Change (T2)
Up-regulated		
Galectin-1	4.1	4.6
p27Kip1	1.8	1.4
Down-regulated		
Metallothionein	0.3	0.1
GSTM-1B (glutathione S-transferase M1B)	0.5	0.4
GST-P1 (glutathione S-transferase P1)	0.6	0.5
Vitronectin	0.5	0.7
Ki-67	0.8	0.6
Integrin αL	0.7	0.7

NOTE. Two core-transgenic mice named T1 and T2 were analyzed.

Table 2. Expression Levels of Differentially Expressed Genes in the Liver of Mice

Gene	Feeding	Core-Transgenic	Nontransgenic	*P* Value*
Galectin-1	normal	3.76 ± 2.65†	1.00 ± 0.38	NS
	ethanol	9.23 ± 5.11	1.13 ± 1.38	<.05
GST-P1	normal	0.85 ± 0.14	1.00 ± 0.42	NS
	ethanol	0.18 ± 0.16	0.55 ± 0.26	<.05
p27Kip1	normal	1.04 ± 0.48	1.00 ± 0.09	NS
	ethanol	1.86 ± 0.55	1.29 ± 1.02	NS

Abbreviation: NS, not statistically significant.

*Mann-Whitney *U* test.

†mRNA copy numbers of each gene quantified by real-time PCR were divided by those of GAPDH and normalized by taking the average value of normal-diet nontransgenic mice as 1 (mean ± SE). The number of mice examined was 4 in each group.

nontransgenic mice with normal diets. Comparing the levels between normal-diet and ethanol-fed mice, expression of GST-P1 was about 5-fold and 2-fold decreased by ethanol in core-transgenic and nontransgenic mice, respectively. Gene expression levels of p27Kip1 were also similar between normal-diet, core-transgenic and nontransgenic mice, but, in ethanol-fed core-transgenic mice, p27Kip1 levels were about 1.5-fold, but not significantly, increased compared with nontransgenic mice (Table 2). This is consistent with the result of the microarray analysis showing a slight increase in core-transgenic mice (Table 1). The core protein and ethanol thus work cooperatively for the modulation of GST-P1 and p27Kip1 mRNA expression.

Protein Expression Levels of Differentially Expressed Genes. The above data derived from microarray analysis were consistent with those from TaqMan RT-PCR analysis examining other pairs of core-transgenic and nontransgenic mice. Consequently, we next examined whether levels of protein expression reflected those with mRNA expression. As expected, galectin-1 expression was increased in ethanol-fed core-transgenic mice, whereas GST-pi, which is encoded by the GST-P1 gene, was decreased (Fig. 5). In addition, protein expression of metallothionein, whose gene expression was the most decreased in ethanol-fed core-transgenic mice (Table 1), was strikingly decreased. The protein expression of these genes thus reflected their differential mRNA expression. On the contrary, expression levels of p27Kip1 protein were rather decreased (Fig. 5), not consistent with mRNA levels (Table 2). Because expression levels of p27Kip1 protein were similar between normal-diet, core-transgenic and nontransgenic mice (data not shown), p27Kip1 protein might have been specifically decreased by ethanol in core-transgenic mice. The investigation of the p27Kip1 degradation mechanism revealed that ERK activation triggers p27Kip1 degradation.[23] Because ERK activity was increased in ethanol-fed core-transgenic mice (Fig. 1), it is suggested that p27Kip1 expression was down-regulated posttranscriptionally via ERK activation in spite of the enhancement of p27Kip1 gene expression compensating for the protein degradation.

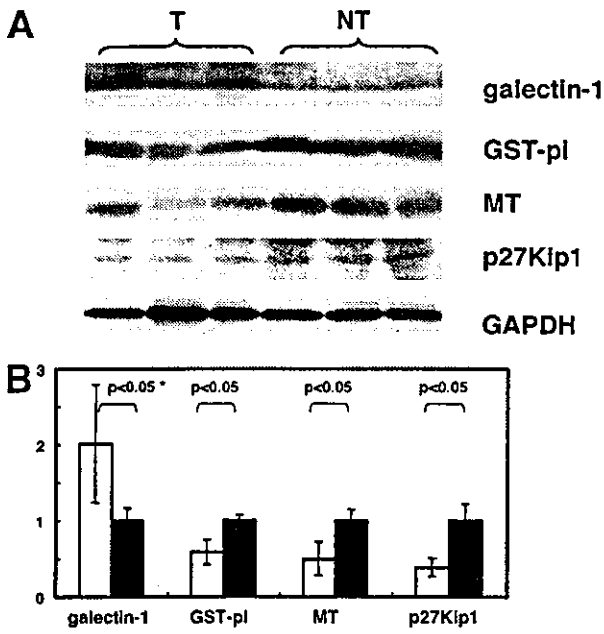

Fig. 5. Protein expression of galectin-1, GST-pi, MT, and p27Kip1 in the liver of ethanol-fed core-transgenic mice. (A) Tissue lysates of the liver of core-transgenic (T) and nontransgenic (NT) mice were separated on a SDS-PAGE gel and immunoblotted for galectin-1, GST-pi, MT, p27Kip1, and GAPDH. (B) Densitometry analysis of the blots shown in (A). **White** and **black columns** indicate core-transgenic and nontransgenic mice, respectively. Values are calculated by dividing the intensity of each band corresponding to the target protein by that of GAPDH and normalized by taking the average intensity of ethanol-fed nontransgenic mice as 1. Data shown are means ± SE. *Mann-Whitney *U* test.

Discussion

In the present study, we demonstrated activation of ERK and p38 MAPK, and their downstream transcription factors, in the liver of core-transgenic mice with ethanol-containing diets. These changes were not observed in core-transgenic mice with normal diets, suggesting that the core protein and ethanol cooperatively activated these MAPK pathways. Activity of JNK, which was activated in normal-diet core-transgenic mice,[16] was similar between ethanol-fed core-transgenic and nontransgenic mice. This is possibly due to the strong effect of ethanol itself on JNK because JNK was very sensitive to various stresses. In fact, ethanol treatment is shown to increase basal JNK activity in liver tissues as well as in primary hepatocytes.[24,25]

Several studies showed the association of the core protein with MAPK activation, especially ERK. However, the results obtained from these studies are somewhat contradictory. The ERK pathway was activated in response to epidermal growth factor in stably core-expressing cells,[26,27] whereas the core protein activated the ERK cascade synergistically with 12-O-tetradecanoyl phorbol 13-acetate but not with epidermal growth factor.[28] On the other hand, Elk-1 but not ERK was activated in response to mitogenic stimuli in cells transiently expressing the core protein.[29] Another recent study showed that the core protein by itself activated ERK as well as JNK and p38 MAPK without extracellular stimuli.[30] Inconsistent effects of the core protein on ERK would be because of the experimental conditions employed, for example, cell culture, systems and levels of the core protein expression, and assay systems. As noted in our recent report,[16] our core-

transgenic mice are a suitable model for investigating effects of the core protein on cellular-signaling pathways including MAPK because expression levels of the core protein in the liver are comparable with that of HCV-infected patients, and their hepatocytes are normal except the core protein expression without inflammatory changes.[31] The present study using this mouse model suggests that the core protein activates ERK in cooperation with ethanol, but only the core protein itself cannot.

It is likely that the core protein and ethanol cooperatively activate ERK and p38 MAPK pathways in transgenic mice. The mechanism of these MAPKs activation is not clearly elucidated, but enhanced ROS generation may be responsible for the activation. The core protein expression itself was shown to induce oxidative stress in some cells.[32] Our analysis also revealed the elevation of hydroperoxide levels and increased activity of antioxidants in core-transgenic mice. This suggests that excessive ROS were generated in our mice by the core protein expression and that generated ROS were promptly scavenged by concomitantly activated antioxidants, leading to balancing redox status.[6] Ethanol, a mild inducer of ROS, however, may stimulate and disrupt this balance, and, possibly, ROS are accumulated, followed by MAPK activation. There are many studies indicating a close relation between MAPK activation and tumor progression. In particular, several studies showed that increased activation of ERK was seen in human HCC as well as rat experimental HCC, suggesting the contribution of ERK activation to HCC development.[33-35] In addition, alcohol intake is one of the synergistic factors to accelerate hepatocarcinogenesis in human chronic hepatitis C.[7-9] Because, in the present study, the mice were fed ethanol-containing diets only for 3 weeks and subsequently killed for analysis at a young age, changes in the rate of HCC development could not be assessed. Furthermore, we could not expect any significant pathologic changes such as necrotic changes and subsequent inflammation and fibrosis. Whether the findings in this study have biologic significance and cause altered hepatocyte phenotype remains to be determined. It is of interest to investigate whether a long-term administration of ethanol accelerates the development of HCC in core-transgenic mice.

We showed that the IKK–NF-κB pathway was not activated in core-transgenic mice. NF-κB is activated by many factors such as cytokines, mitogens, and viral proteins.[36] As for HCV core protein, however, there are several conflicting data concerning NF-κB activation. It is known that NF-κB is activated by ROS. Therefore, it was unexpected that NF-κB was not activated in these ethanol-fed core-transgenic mice, in which we observed an increase in ROS. One possible explanation is that an inhibitory mechanism works upstream of IKK in the core-expressing cells. As we and other researchers reported previously, the core protein itself acts as an inducer of intracellular oxidative stress, and hepatocytes in turn protect themselves by up-regulating cellular antioxidant defense mechanisms.[6,32] In view of these findings, some antioxidant actions may contribute to repressing NF-κB activation in ROS-accumulated core-expressing cells. Otherwise, levels of generated ROS in ethanol-fed core-transgenic mice were low so that NF-κB was not activated. In fact, a low-level oxidative stress was shown to selectively activate p38 MAPK but not NF-κB cascade.[11]

We found that 8 mRNA out of 434 cancer-related genes were altered in abundance, 2 up-regulated and 6 down-regulated, in the liver of ethanol-fed core-transgenic mice. The most decreased 3 genes, metallothionein, GST-M1B, and GST-P1, are all so-called antioxidant-related genes. The metallothioneins are low-molecular-weight, cysteine-rich metalloproteins shown to be a potent oxygen radical scavenger and can protect cells from oxidative stress.[37] GSTs are detoxification enzymes engaged in catalyzing the conjugation of glutathione with electrophilic compounds and play a key role in the protection against oxidative stress.[38] Therefore, one can easily speculate that down-regulated expression of these genes in hepatocytes causes reduced protection from ROS and that cells are more sensitive to oxidative stress, possibly leading to several pathogeneses including HCC. In fact, GST as well as metallothionein was down-regulated in human HCC.[39,40] We also showed that expression of vitronectin and integrin αL was decreased in ethanol-fed core-transgenic mice (Table 1). These proteins work for cell-cell and cell-matrix interaction and are closely associated with regulation of cell morphology and cell proliferation.[41] Interestingly, vitronectin expression was down-regulated in chronically HCV-infected human livers as well as moderately/poorly differentiated HCC.[42,43] Therefore, repressed expression of these genes may also contribute to the pathogenesis of HCV infection in human livers.

Galectin-1 is the gene most strikingly up-regulated in ethanol-fed core-transgenic mice. Further analysis by TaqMan RT-PCR showed that expression of galectin-1 tended to be increased also in normal-diet core-transgenic mice, although not statistically significant. This suggests that the core protein itself potentially enhances galectin-1 gene expression and that this enhancement is accelerated by ethanol feeding. The mechanism of the up-regulation of the galectin-1 gene remains to be elucidated, but we are now examining whether the promoter activity of the galectin-1 gene is enhanced in core-expressing cells. Expression of galectin-1 is known to be controlled by DNA

methylation in the promoter region containing clusters of CpG dinucleotides.[44] Notably, a recent study showed that oxidative DNA damage promotes CG→TT tandem mutations at methylated CpG dinucleotides.[45] Considering these findings, expression of galectin-1 may be modulated through the changes in methylated CpG sequences by oxidative stress generated in core-transgenic mice. Galectin-1 appears to play key roles in different biologic processes, such as cell differentiation and growth control, cell-cell and cell-matrix interactions, and tumor progression.[46] A recent interesting study indicated that galectin-1 binds to oncogenic H-Ras and increases membrane-associated Ras, Ras-GTP, and active ERK, resulting in cell transformation.[20] Considering this report, although the present study could not demonstrate the association of galectin-1 with ERK pathway activation, expression of galectin-1 triggers the hepatocyte transformation and may, at least in part, contribute to HCC development in core-transgenic mice, which may be accelerated by ethanol feeding. At this point, we are now investigating whether hepatocytes in ethanol-fed core-transgenic mice are more proliferative or vulnerable to transformation.

In contrast to the up-regulation of p27Kip1 gene expression, p27Kip1 protein was decreased in ethanol-fed core-transgenic mice. Considering the previous report showing that p27Kip1 degradation is accelerated by ERK activation,[24] a slight increase in p27Kip1 mRNA might compensate for the accelerated protein degradation. p27Kip1 binds and inhibits cyclin-dependent kinase2/cyclinE and enforces the G1 restriction point.[47] A large number of clinical studies have linked a poor survival prognosis with low levels and reduced half-life of the p27Kip1 protein in many tumor types.[48,49] In addition, multiple-organ hyperplasia and pituitary tumors are observed in p27-deficient mice.[50] These findings indicate that a loss or decrease of p27Kip1 protein expression links to the tumorigenesis and progression. Therefore, the decreased expression of p27Kip1 protein may be associated with HCC development in human HCV-infected livers as well as in core-transgenic mice.

In conclusion, our results indicate that HCV core protein activates ERK and p38 MAPK cooperatively with ethanol and modulates the expression of several genes related to cell transformation, cell cycle, and antioxidants in a mouse model for HCV-associated HCC. Further study is necessary to demonstrate whether these changes contribute to significant pathologic changes and actually occurred in HCV-infected livers, but data in the present study may give a clue to the understanding of molecular mechanisms of HCV-related pathogenesis associated with ethanol consumption in human livers.

Acknowledgment: The authors thank their colleagues for helpful discussion and M. Matsuda and M. Yahata for their technical assistance.

References

1. Saito I, Miyamura T, Ohbayashi A, Harada H, Katayama T, Kikuchi S, Watanabe Y, et al. Hepatitis C virus infection is associated with the development of hepatocellular carcinoma. Proc Natl Acad Sci U S A 1990;87: 6547-6549.
2. Tarao K, Rino Y, Ohkawa S, Tamai S, Miyakawa K, Takakura H, Endo O, et al. Close association between high serum alanine aminotransferase levels and multicentric hepatocarcinogenesis in patients with hepatitis C virus-associated cirrhosis. Cancer 2002;94:1787-1795.
3. Tanaka H, Tsukuma H, Yamano H, Okubo Y, Inoue A, Kasahara A, Hayashi N. Hepatitis C virus 1b infection and development of chronic hepatitis, liver cirrhosis and hepatocellular carcinoma: a case-control study in Japan. J Epidemiol 1998;8:244-249.
4. Suzuki R, Suzuki T, Ishii K, Matsuura Y, Miyamura T. Processing and functions of hepatitis C virus proteins. Intervirology 1999;42:145-152.
5. Moriya K, Fujie H, Shintani Y, Yotsuyanagi H, Tsutsumi T, Ishibashi K, Matsuura Y, et al. The core protein of hepatitis C virus induces hepatocellular carcinoma in transgenic mice. Nat Med 1998;4:1065-1067.
6. Moriya K, Nakagawa K, Santa T, Shintani Y, Fujie H, Miyoshi H, Tsutsumi T, et al. Oxidative stress in the absence of inflammation in a mouse model for hepatitis C virus-associated hepatocarcinogenesis. Cancer Res 2001;61:4365-4370.
7. Ikeda K, Saitoh S, Koida I, Arase Y, Tsubota A, Chayama K, Kumada H, et al. A multivariate analysis of risk factors for hepatocellular carcinogenesis: a prospective observation of 795 patients with viral and alcoholic cirrhosis. HEPATOLOGY 1993;18:47-53.
8. Yoshihara H, Noda K, Kamada T. Interrelationship between alcohol intake, hepatitis C, liver cirrhosis, and hepatocellular carcinoma. Recent Dev Alcohol 1998;14:457-469.
9. Donato F, Tagger A, Chiesa R, Ribero ML, Tomasoni V, Fasola M, Gelatti U, et al. Hepatitis B and C virus infection, alcohol drinking, and hepatocellular carcinoma: a case-control study in Italy. Brescia HCC Study. HEPATOLOGY 1997;26:579-584.
10. Cross TG, Scheel-Toellner D, Henriquez NV, Deacon E, Salmon M, Lord JM. Serine/threonine protein kinases and apoptosis. Exp Cell Res 2000; 256:34-41.
11. Kurata S. Selective activation of p38 MAPK cascade and mitotic arrest caused by low level oxidative stress. J Biol Chem 2000;275:23413-23416.
12. Gupta A, Rosenberger SF, Bowden GT. Increased ROS levels contribute to elevated transcription factor and MAP kinase activities in malignantly progressed mouse keratinocyte cell lines. Carcinogenesis 1999;20:2063-2073.
13. Herrera B, Fernandez M, Roncero C, Ventura JJ, Porras A, Valladares A, Benito M, et al. Activation of p38MAPK by TGF-β in fetal rat hepatocytes requires radical oxygen production, but is dispensable for cell death. FEBS Lett 2001;499:225-229.
14. Ikeyama S, Kokkonen G, Shack S, Wang XT, Holbrook NJ. Loss in oxidative stress tolerance with aging linked to reduced extracellular signal-regulated kinase and Akt kinase activities. FASEB J 2002;16:114-116.
15. Moriya K, Yotsuyanagi H, Shintani Y, Fujie H, Ishibashi K, Matsuura Y, Miyamura T, et al. Hepatitis C virus core protein induces hepatic steatosis in transgenic mice. J Gen Virol 1997;78:1527-1531.
16. Tsutsumi T, Suzuki T, Moriya K, Yotsuyanagi H, Shintani Y, Fujie H, Matsuura Y, et al. Alteration of intrahepatic cytokine expression and AP-1 activation in transgenic mice expressing hepatitis C virus core protein. Virology 2002;304:415-424.
17. Payne DM, Rossomando AJ, Martino P, Erickson AK, Her JH, Shabanowitz J, Hunt DF, et al. Identification of the regulatory phosphorylation sites in pp42/mitogen-activated protein kinase. EMBO J 1991;10: 885-892.
18. Raingeaud J, Gupta S, Rogers JS, Dickens M, Han J, Ulevitch RJ, Davis RJ. Pro-inflammatory cytokines and environmental stress cause p38 mito-

gen-activated protein kinase activation by dual phosphorylation on tyrosine and threonine. J Biol Chem 1995;270:7420-7426.
19. Marais R, Wynne J, Treisman R. The SRF accessory protein Elk-1 contains a growth factor-regulated transcriptional activation domain. Cell 1993;73:381-393.
20. Elad-Sfadia G, Haklai R, Ballan E, Gabius HJ, Kloog Y. Galectin-1 augments Ras activation and diverts Ras signals to Raf-1 at the expense of phosphoinositide 3-kinase. J Biol Chem 2002;277:37169-37175.
21. Mayr B, Montminy M. Transcriptional regulation by the phosphorylation-dependent factor CREB. Nat Rev Mol Cell Biol 2001;2:599-609.
22. Sementchenko VI, Watson DK. Ets target genes: past, present and future. Oncogene 2000;19:6533-6548.
23. Delmas C, Manenti S, Boudjelal A, Peyssonnaux C, Eychene A, Darbon JM. The p42/p44 mitogen-activated protein kinase activation triggers p27Kip1 degradation independently of CDK2/cyclin E in NIH 3T3 cells. J Biol Chem 2001;276:34958-34965.
24. Chen J, Ishac EJ, Dent P, Kunos G, Gao B. Effects of ethanol on mitogen-activated protein kinase and stress-activated protein kinase cascades in normal and regenerating liver. Biochem J 1998;334:669-676.
25. Chung J, Chavez PR, Russell RM, Wang XD. Retinoic acid inhibits hepatic Jun N-terminal kinase-dependent signaling pathway in ethanol-fed rats. Oncogene 2002;21:1539-1547.
26. Tsuchihara K, Hijikata M, Fukuda K, Kuroki T, Yamamoto N, Shimotohno K. Hepatitis C virus core protein regulates cell growth and signal transduction pathway transmitting growth stimuli. Virology 1999;258: 100-107.
27. Giambartolomei S, Covone F, Levrero M, Balsano C. Sustained activation of the Raf/MEK/Erk pathway in response to EGF in stable cell lines expressing the hepatitis C virus (HCV) core protein. Oncogene 2001;20: 2606-2610.
28. Hayashi J, Aoki H, Kajino K, Moriyama M, Arakawa Y, Hino O. Hepatitis C virus core protein activates the MAPK/ERK cascade synergistically with tumor promoter TPA, but not with epidermal growth factor or transforming growth factor α. HEPATOLOGY 2000;32:958-961.
29. Fukuda K, Tsuchihara K, Hijikata M, Nishiguchi S, Kuroki T, Shimotohno K. Hepatitis C virus core protein enhances the activation of the transcription factor, Elk1, in response to mitogenic stimuli. HEPATOLOGY 2001;33:159-165.
30. Erhardt A, Hassan M, Heintges T, Haussinger D. Hepatitis C virus core protein induces cell proliferation and activates ERK, JNK, and p38 MAP kinases together with the MAP kinase phosphatase MKP-1 in a HepG2 Tet-Off cell line. Virology 2002;292:272-284.
31. Koike K, Tsutsumi T, Fujie H, Shintani Y, Kyoji M. Molecular mechanism of viral hepatocarcinogenesis. Oncology 2002;62(Suppl 1):29-37.
32. Li K, Prow T, Lemon SM, Beard MR. Cellular response to conditional expression of hepatitis C virus core protein in Huh7 cultured human hepatoma cells. HEPATOLOGY 2002;35:1237-1246.
33. McKillop IH, Schmidt CM, Cahill PA, Sitzmann JV. Altered expression of mitogen-activated protein kinases in a rat model of experimental hepatocellular carcinoma. HEPATOLOGY 1997;26:1484-1491.
34. Ito Y, Sasaki Y, Horimoto M, Wada S, Tanaka Y, Kasahara A, Ueki T, et al. Activation of mitogen-activated protein kinases/extracellular signal-regulated kinases in human hepatocellular carcinoma. HEPATOLOGY 1998;27: 951-958.
35. Schmidt CM, McKillop IH, Cahill PA, Sitzmann JV. Increased MAPK expression and activity in primary human hepatocellular carcinoma. Biochem Biophys Res Commun 1997;236:54-58.
36. Baeuerle PA. The inducible transcription activator NF-κB: regulation by distinct protein subunits. Biochim Biophys Acta 1991;1072:63-80.
37. Sato M, Bremner I. Oxygen free radicals and metallothionein. Free Radic Biol Med 1993;14:325-337.
38. Mannervik B, Alin P, Guthenberg C, Jensson H, Tahir MK, Warholm M, Jornvall H. Identification of three classes of cytosolic glutathione transferase common to several mammalian species: correlation between structural data and enzymatic properties. Proc Natl Acad Sci U S A 1985;82: 7202-7206.
39. Okabe H, Satoh S, Kato T, Kitahara O, Yanagawa R, Yamaoka Y, Tsunoda T, et al. Genome-wide analysis of gene expression in human hepatocellular carcinomas using cDNA microarray: identification of genes involved in viral carcinogenesis and tumor progression. Cancer Res 2001;61:2129-2137.
40. Xu XR, Huang J, Xu ZG, Qian BZ, Zhu ZD, Yan Q, Cai T, et al. Insight into hepatocellular carcinogenesis at transcriptome level by comparing gene expression profiles of hepatocellular carcinoma with those of corresponding noncancerous liver. Proc Natl Acad Sci U S A 2001;98:15089-15094.
41. Hynes RO. Integrins: versatility, modulation, and signaling in cell adhesion. Cell 1992;69:11-25.
42. Honda M, Kaneko S, Kawai H, Shirota Y, Kobayashi K. Differential gene expression between chronic hepatitis B and C hepatic lesion. Gastroenterology 2001;120:955-966.
43. Delpuech O, Trabut JB, Carnot F, Feuillard J, Brechot C, Kremsdorf D. Identification, using cDNA macroarray analysis, of distinct gene expression profiles associated with pathological and virological features of hepatocellular carcinoma. Oncogene 2002;21:2926-2937.
44. Benvenuto G, Carpentieri ML, Salvatore P, Cindolo L, Bruni CB, Chiariotti L. Cell-specific transcriptional regulation and reactivation of galectin-1 gene expression are controlled by DNA methylation of the promoter region. Mol Cell Biol 1996;16:2736-2743.
45. Lee DH, O'Connor TR, Pfeifer GP. Oxidative DNA damage induced by copper and hydrogen peroxide promotes CG→TT tandem mutations at methylated CpG dinucleotides in nucleotide excision repair-deficient cells. Nucleic Acids Res 2002;30:3566-3573.
46. Barondes SH, Cooper DN, Gitt MA, Leffler H. Galectins. Structure and function of a large family of animal lectins. J Biol Chem 1994;269:20807-20810.
47. Polyak K, Kato JY, Solomon MJ, Sherr CJ, Massague J, Roberts JM, Koff A. p27Kip1, a cyclin-Cdk inhibitor, links transforming growth factor-β and contact inhibition to cell cycle arrest. Genes Dev 1994;8:9-22.
48. Sgambato A, Cittadini A, Faraglia B, Weinstein IB. Multiple functions of p27(Kip1) and its alterations in tumor cells: a review. J Cell Physiol 2000; 183:18-27.
49. Slingerland J, Pagano M. Regulation of the cdk inhibitor p27 and its deregulation in cancer. J Cell Physiol 2000;183:10-17.
50. Nakayama K, Ishida N, Shirane M, Inomata A, Inoue T, Shishido N, Horii I, et al. Mice lacking p27(Kip1) display increased body size, multiple organ hyperplasia, retinal dysplasia, and pituitary tumors. Cell 1996;85: 707-720.

JOURNAL OF VIROLOGY, Nov. 2002, p. 11775–11779 Vol. 76, No. 22
0022-538X/02/$04.00+0 DOI: 10.1128/JVI.76.22.11775–11779.2002

Diverging Effects of Human Recombinant Anti-Hepatitis C Virus (HCV) Antibody Fragments Derived from a Single Patient on the Infectivity of a Vesicular Stomatitis Virus/HCV Pseudotype

Roberto Burioni,[1]* Yoshiharu Matsuura,[2] Nicasio Mancini,[1] Hideki Tani,[2] Tatsuo Miyamura,[3] Pietro E. Varaldo,[1] and Massimo Clementi[4]

Institute of Microbiology, University of Ancona, 60020 Ancona,[1] and Università "Vita-Salute San Raffaele," IRCCS Istituto Scientifico San Raffaele, 20132 Milan,[4] Italy, and Research Center for Emerging Infectious Diseases and Research Institute for Microbial Diseases, Osaka University, Osaka 565-0871,[2] and Department of Virology II, National Institute of Infectious Diseases, Tokyo,[3] Japan

Received 20 March 2002/Accepted 8 August 2002

Hepatitis C virus (HCV) is the major causative agent of blood-borne non-A, non-B hepatitis. Although a strong humoral response is detectable within a few weeks of primary infection and during viral persistence, the role played by antibodies against HCV envelope glycoproteins in controlling viral replication is still unclear. We describe how human monoclonal anti-HCV E2 antibody fragments isolated from a chronically HCV-infected patient differ sharply in their abilities to neutralize infection of HepG2 cells by a vesicular stomatitis virus pseudotype bearing HCV envelope glycoproteins. Two clones were able to neutralize the pseudotype virus at a concentration of 10 μg/ml, while three other clones completely lacked this activity. These data can explain the lack of protection and the possibility of reinfection that occur even in the presence of a strong antiviral antibody response.

Hepatitis C virus (HCV) is the major causative agent of blood-borne non-A, non-B hepatitis (10), infecting more than 200 million people worldwide (3). The tendency of HCV infection toward chronicity (8), with persistent viral replication (3), suggests that the host immune response is unable to tackle and eradicate the infection in the majority of cases. The role of the humoral response against viral envelope glycoproteins (E1 and E2) in the control of viral replication is still unclear (8). The study and demonstration of neutralizing antibodies have been hampered by the lack of a robust neutralization system, by the paucity of animal models, and by the differences between human and animal antibody responses to HCV antigens (1, 4). To investigate the effects of human antibodies on key viral steps such as viral entry into target cells, we used a model that reproduces HCV infection by means of vesicular stomatitis virus (VSV) pseudotypes bearing HCV envelope glycoproteins (VSV/HCV). A recombinant VSV, in which the glycoprotein (G) gene had been replaced with a reporter gene (VSVΔG*) encoding green fluorescent protein (GFP), was used to produce VSV/HCV pseudotypes possessing the HCV E1 and E2 envelope glycoproteins (13). The infectivity of pseudotypes can be determined by quantifying the number of cells expressing the GFP reporter gene using fluorescence microscopy. Briefly, the VSVΔG*/HCVE1-E2 pseudotype (VSV/HCV) consisted of VSV in which the G envelope protein was replaced with chimeric HCV E1 and E2 envelope glycoproteins consisting of the ectodomains of E1 and E2 proteins of a type 1b HCV cDNA clone (NIH-J1) (2) fused to the N-terminal signal sequences, transmembrane, and cytoplasmic domain of VSV G protein (13, 15, 19). VSV/HCV pseudotypes were prepared by infecting CHO cells with a VSV in which the G protein-coding region had been replaced with GFP (18). The VSVΔG*/G pseudotype (VSV/G), used as a control (as well as to produce the VSV/HCV pseudotype), was produced by infecting a cell line transiently expressing G protein with VSVΔG*. To determine whether the chimeric proteins could be incorporated into VSV particles, the CHO cell line expressing E1 and E2 on its surface was infected with VSVΔG*/G. After 16 h, the infected cell supernatant was collected and the pseudotyped viruses were purified by centrifugation through sucrose density gradients and analyzed by immunoblotting (13). VSVΔG*/G and VSVΔG* were produced as controls by infecting CHO cells transiently expressing VSV G protein or the parental CHO cells with VSVΔG*/G. The VSV structural proteins N, P, and M (matrix protein) were present in all of the purified virions. VSV G protein was detected in VSVΔG*/G but not in VSVΔG*-negative controls or in the HCV pseudotype virus (13). Virions produced in cells expressing the chimeric HCV envelope proteins contained both E1 and E2, indicating that HCV glycoproteins were correctly assembled into VSV particles. The relative infectivities of VSVΔG*/G and VSVΔG*/HCVE1-E2 for HepG2 cells were comparable in experiments repeated with 3 different batches of viruses (13).

To evaluate the efficiency of the humoral anti-HCV immune response in inhibiting viral entry into cells, we examined whether the pseudotypes could be neutralized by a panel of human monoclonal antibody Fab fragments derived from a phage display repertoire library containing the immunoglobulin G1 kappa (IgG1κ) repertoire of a patient chronically infected with HCV of type 1b (7). The antibody fragments, selected with purified recombinant HCV/E2 of type 1a (strain

* Corresponding author. Mailing address: Servizio di Virologia, Istituto di Microbiologia, Facoltà di Medicina e Chirurgia, Università di Ancona, Via Conca, 60020 Ancona, Italy. Phone: 39 335 8349277. Fax: 39 071 5964850. E-mail: r.burioni@libero.it.

TABLE 1. Germ lines and V gene mutations in variable regions of anti-HCV E2 human monoclonal antibodies[a]

Polypeptide chain	Antibody	V gene	% of mutated nucleotides in:		% of mutated amino acids in:	
			FRs	CDRs	FRs	CDRs
Heavy	e8	VH1-18	9.5	22.2	14.9	33.3
	e20	VH1-69	9.4	16.9	19	38
	e137	VH1-69	11.5	15.3	14	41.7
	e301	VH1-69	8.9	19.4	15.6	45.8
	e509	VH1-69	5.2	15.9	10.9	33.3
Light	e8	KV3-20	2.7	16	2.6	33.3
	e20	KV1-9	4.3	7.7	9.7	22.2
	e137	KV1-8	2.2	9	3.2	15.4
	e301	KV3-15	3.8	14.3	9.7	23
	e509	KV3-15	3.2	1.3	6.5	0

[a] Sequences were determined as described previously (7) and aligned with germ line sequences in the IMGT database (11). The percentages of nucleotide and amino acid mutations were calculated according to the alignment method of Kabat et al. (9), taking into account framework regions (FRs) 1, 2, and 3 for heavy and light chains and complementarity-determining regions (CDRs) 1 and 2 for heavy chains and 1, 2, and 3 for light chains.

H) (12) expressed in CHO cells, have been fully characterized and have been demonstrated to correspond to clones actually present in the serum of chronically infected patients (4). All Fabs demonstrated similar affinity for the E2 antigen, with monomer Fab antigen binding constants on the order of 10^7 to 10^8 mol/liter^{-1} (7). Each of the five antibodies used in this study represents one of the five families in which the whole anti-E2 antibody repertoire of this patient was grouped. Fabs belonging to the same family share similar biological activities and have strong homologies of DNA sequences (7). Extensive competition studies have demonstrated that these antibody fragments recognize five different epitopes on the surface of the E2 glycoprotein (4). Epitope mapping of these Fabs was carried out by means of a peptide scan using 15-amino-acid long overlapping peptides, covering the whole sequence of the E2 protein, for selection and screening. Fabs did not show any reaction (7), indicating their recognition of the conformational epitopes that are not reproduced in the peptide scan approach. Immunoprecipitation experiments were carried out to demonstrate specific binding of human recombinant Fabs to VSV/HCV pseudoviruses. Briefly, 10 μl of the purified pseudovirus preparation described above was incubated for 4 h at 37°C with FLAG-tagged purified human recombinant Fabs (5) at a final concentration of 20 ng/μl; after this step, 40 μl of anti-FLAG M2 affinity gel (Sigma, Saint Louis, Mo.), consisting of a purified murine IgG1 monoclonal antibody specifically recognizing the FLAG epitope covalently attached to agarose, was added and the mixture was incubated overnight at 4°C with gentle shaking. After this step, the resin was washed five times at 4°C with phosphate-buffered saline (PBS) with 0.5% fetal bovine serum, followed by 15 washes with PBS alone. Viral RNA that might have been present in the pellet was extracted and demonstrated by reverse transcription-PCR with a modification of established methods (14). Briefly, VSV RNA in the pellet was retrotranscribed with the primer IS (5′-GGTGTTG CAGACTATGTTGGAC-3′), and the cDNA thus obtained was amplified by PCR (denaturation at 93°C for 1 min, annealing at 37°C for 1 min, and extension at 72°C for 2 min, repeated for 35 cycles) with the IS primer and the IA primer (5′-GGT GTTGCAGACTATGTTGAC-3′). The expected 395-bp DNA derived from correct amplification of the VSV genome was demonstrated in a 2% agarose gel. All human anti-HCV E2 Fabs precipitated the VSV/HCV pseudotypes but not the VSV/G controls. No precipitation was demonstrated with a control Fab (6) or in control tubes where no FLAG-tagged Fab was added. In enzyme-linked immunosorbent assay inhibition studies with sera derived from HCV-positive patients (4), the human recombinant monoclonal Fabs used in this study were demonstrated to be not artifacts but representative of clones existing in the human anti-HCV immunoresponse.

Divergences of variable-region DNA sequences from the relative germ line sequences are typical of antigen-driven affinity maturation (Table 1), suggesting a prolonged exposure to the antigen.

The neutralization of binding (NOB) activity of each Fab was also determined as described previously (7, 17). Briefly, 20 μl of E2 glycoprotein (0.5 μg/ml in PBS) was mixed with progressive dilutions of purified Fab preparations in 96-well U-bottom microplates. After incubation at 4°C for 1 h, pellets of MOLT-4 cells (10^5/well) were added and incubated for 1 h at 4°C. Unbound HCV proteins and antibodies were removed by two centrifugations in PBS at 200 ×*g* for 5 min at 4°C. Cells were subsequently incubated for 30 min at 4°C with human polyclonal anti-HCV E2 serum at a 1/100 dilution. Cells were washed twice in PBS and incubated for 30 min at 4°C with fluorescein isothiocyanate-labeled goat anti-human IgG at a 1/100 dilution. Cells were washed as described above and resuspended in 100 μl of PBS; cell-bound fluorescence was analyzed with a FACScan flow cytometer (Becton Dickinson, Sparks, Md.) and evaluated as described above. The concentrations at which NOB and 50% NOB were achieved were calculated as described previously (7, 17). The results clearly indicated that some clones (e137 and e8) were unable to inhibit HCV E2 binding to cells and that others inhibited binding even at very low concentrations (Table 2). Evaluation of the NOB of pseudotyped viruses to CD81 was not possible due to the very low binding of VSV/HCV to this molecule compared to the background (R. Burioni and Y. Matsuura, unpublished observation).

The pseudotype neutralization assay performed was a modification of a previously described method (13). Briefly, dilutions of purified human recombinant Fabs were incubated with 2.4×10^3 infectious units of the VSV/HCV or VSV/G pseudotype for 30 min at 37°C and inoculated into HepG2 cells (4

TABLE 2. Neutralization of E2 binding to target cell and of VSV/HCV entry into hepatoma cells by the human recombinant anti-E2 Fabs used in this study

Fab clone	50% NOB concentration (μg/ml) (relative level of NOB activity)[a]	Effect on VSV/HCV infection
e8	>40 (none)	None
e20	3 (high)	None
e137	40 (low)	Inhibition
e301	3 (high)	Strong inhibition
e509	<0.035 (highest)	Enhancement

[a] NOB activity data are derived from data previously published (7).

$\times 10^4$ cells) prepared in a 96-well plate. After adsorption for 60 min at 37°C, the cells were washed three times with Dulbecco's modified Eagle medium containing 10% fetal bovine serum and incubated at 37°C for 16 h; then, the number of infectious units of virus was determined by counting the number of GFP-expressing cells by fluorescence microscopy. The data are presented as the percentages of inhibition compared with the results from control wells to which no antibody was added and represent the average of three experiments performed in duplicate.

Two of the Fabs, e8 and e20, recognizing different epitopes on the surface of HCV E2 (4), did not neutralize VSV/HCV pseudotype infection (data not shown) even at the highest concentration used (80 μg/ml). Remarkably, one of these two Fabs, e20, was demonstrated to have strong NOB activity (7), confirming the notion that even antibodies inhibiting E2 binding may fail to prevent viral infection.

Two other Fabs, e137 and e301, efficiently neutralized VSV/HCV at a concentration of 10 μg/ml, while VSV pseudotypes bearing the VSV G envelope protein (VSV/G pseudotypes) were not affected (Fig. 1a and b). These data are congruent with previous findings (4) indicating that these two clones compete for the same E2 region, probably recognized by human antibodies endowed with neutralizing activity, as shown in a two-dimensional surface map of the human epitopes on HCV E2 (Fig. 2).

Fab e509 is currently the strongest available antibody in terms of NOB activity, inhibiting binding between E2 and the cellular target at a very low concentration (Table 2). Incubation of VSV/HCV pseudotypes with this Fab at concentrations as low as 1 μg/ml apparently enhanced virus entry into hepatoma cells. No increase in infectivity was demonstrated when VSV/G pseudotypes were used, thus ruling out the possibility that a nonspecific interaction between this Fab and the cellular membrane promoted viral entry into the cell (Fig. 1c).

A control antibody (6) exerted no effect on the pseudotype system, as it failed to neutralize both VSV/HCV and VSV/G pseudotypes (data not shown). The VSV/G pseudotype was duly neutralized by a polyclonal anti-VSV antiserum at dilutions of up to 1:1,000 used as a neutralization control in these experiments (13), which had no effect on VSV/HCV (data not shown). Since a neutralizing effect was first demonstrated in the present work, a neutralizing control for VSV/HCV pseudotypes was not available. Polyclonal and monoclonal anti-E1 and anti-E2 antibodies raised in several hosts showed no neutralizing effect on VSV/HCV pseudotypes (Y. Matsuura, unpublished data)

Several aspects of the data presented here deserve special attention. First, the neutralizing activity of monovalent Fabs showed that HCV entry can be inhibited without the need for virion aggregation or cross-linking; furthermore, it is unlikely that the blocking of the interaction between the virus and its cellular target is a key factor in HCV neutralization, reinforcing the growing skepticism about CD81 playing a crucial role in HCV entry in susceptible cells. These data can explain at the molecular level the lack of correlation between NOB activity in the serum and protection from disease. Since the antibodies were elicited by epitopes exposed during natural infection, they are unlikely to be artifacts created by epitopes present only on recombinant proteins, as demonstrated by the inhibition of

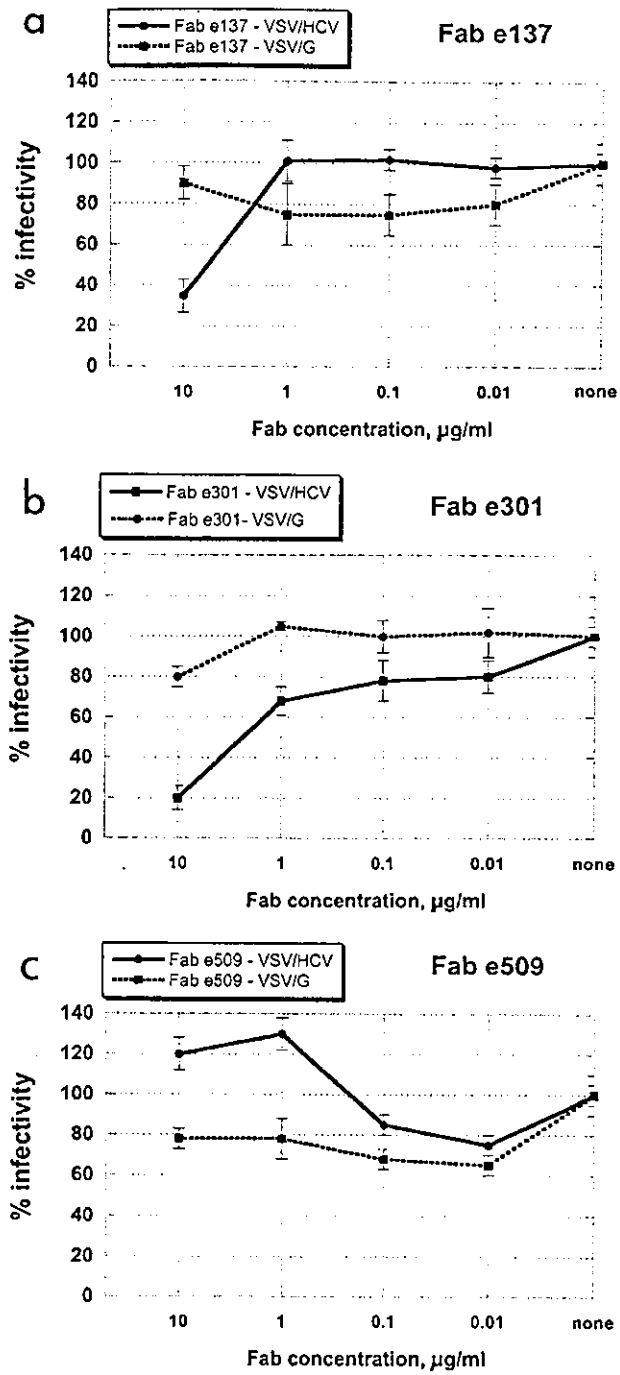

FIG. 1. Inhibition of infection of VSV/HCV and VSV/G pseudotypes by purified anti-HCV E2 human recombinant Fabs e137 (a), e301 (b), and e509 (c) at different concentrations. HepG2 cells infected with Fab-treated pseudotypes were incubated for 16 h, and the number of GFP-expressing cells was determined by fluorescence microscopy. Data are presented as percentages of the infection detected in control wells (no Fabs added). The results shown are the average of three independent assays performed in duplicate, with error bars representing standard deviations.

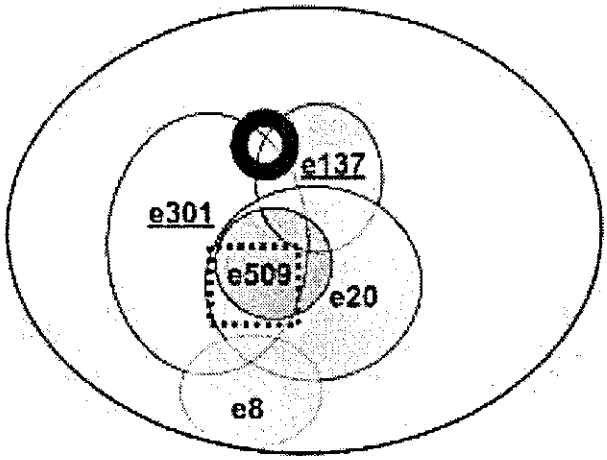

FIG. 2. Two-dimensional surface-like map of the human B-cell epitopes present on the surface of HCV E2, as recognized by the monoclonal antibodies used in this study. Overlapping circles indicate reciprocal inhibition. Fabs endowed with VSV/HCV pseudotype-neutralizing activity are underlined. The putative region mediating the interaction between HCV E2 and the cellular target is indicated by the dotted-line square. The putative region recognized by neutralizing antibodies is indicated by a thick black circle. Due to modifications that can be induced by antigen-antibody interactions, this diagram does not correspond to the actual physical map. The map without neutralization data is derived from previously published work (4).

their binding to HCV E2 with sera derived from HCV-positive patients (4). Finally, we demonstrate that some degree of cross-protection is provided by anti-HCV antibodies. Although formal proof of the cross-reactivity of our Fabs with E2 of a type different from 1a was not provided due to the difficulty of obtaining purified E2 of other types, antibodies selected with E2 of type 1a were able to neutralize and immunoprecipitate a pseudotype bearing E2 of type 1b.

Another finding described in this paper is that Fab e509 was able to enhance the infectivity of the VSV/HCV pseudotype virus, although no effect on the VSV/G construct was apparent. Even though further studies are needed to conclusively demonstrate this activity, Fab e509 seems to be an important tool to use in studying the interactions between HCV and the cell surface.

The observation that, out of a panel of human Fabs derived from an infected patient, two Fabs were able to inhibit viral entry, two were not influential, and one promoted infection can help us to understand how HCV escapes the control of the immune system. These data strongly suggest that a part of the effort of the immune system may be directed toward the production of antibodies that are not necessarily beneficial to the host. Given that antibodies able to inhibit the antigen binding of these Fabs have been isolated in the sera of patients, and that an excess of these Fabs can inhibit serum binding to E2 by more than 70% (4), the artifactual nature of the Fabs used in this study can be ruled out. Assays able to quantify the amount of antibodies directed against the different epitopes in the sera of patients (R. Burioni, submitted for publication) will make it possible to demonstrate whether the amount of antibodies directed against each epitope correlates with a different outcome of the viral infection.

Finally, the results shown here will help in the design of possible vaccine strategies and their in vitro evaluation (16). This would be a considerable advance in the case of an infection lacking an animal model. Molecules demonstrated in vitro to selectively stimulate the production of neutralizing antibodies but not to elicit the production of immunoglobulins that are not beneficial to the host will be the best candidates for further in vivo studies.

R.B. and Y.M. contributed equally to this paper.

We thank A. Grieco, G. Malcangi, S. Bighi, M. Perotti, S. Bellagamba, S. Carletti, and M. Vecchi for their valuable assistance. R.B. is deeply grateful to Giovanni Gasbarrini for critical help and continuous support.

This work was supported by grants from Istituto Superiore di Sanità to R.B. and M.C.

REFERENCES

1. **Ahmed, M., T. Shikata, and M. Esumi.** 1996. Murine humoral immune response against recombinant structural proteins of hepatitis C virus distinct from those of patients. Microbiol. Immunol. 40:169–176.
2. **Aizaki, H., Y. Aoki, T. Harada, K. Ishii, T. Suzuki, S. Nagamori, G. Toda, Y. Matsuura, and T. Miyamura.** 1998. Full-length complementary DNA of hepatitis C virus genome from an infectious blood sample. Hepatology 27: 621–627.
3. **Alter, M. J., H. S. Margolis, K. Krawczynski, F. N. Judson, A. Mares, W. J. Alexander, P. Y. Hu, J. K. Miller, M. A. Gerber, R. E. Sampliner, et al.** 1992. The natural history of community-acquired hepatitis C in the United States. N. Engl. J. Med. 327:1899–1905.
4. **Bugli, F., N. Mancini, C.-Y. Kang, C. Di Campli, A. Grieco, A. Manzin, A. Gabrielli, A. Gasbarrini, G. Fadda, P. E. Varaldo, M. Clementi, and R. Burioni.** 2001. Mapping B-cell epitopes of hepatitis C virus E2 glycoprotein using human monoclonal antibodies from phage display libraries. J. Virol. 75:9986–9990.
5. **Burioni, R., F. Bugli, N. Mancini, and G. Fadda.** 2001. A novel expression vector for production of epitope-tagged recombinant Fab fragments in bacteria. Hum. Antibodies 10:149–154.
6. **Burioni, R., P. Plaisant, F. Bugli, L. Solforosi, V. D. Carri, P. E. Varaldo, and G. Fadda.** 1998. A new subtraction technique for molecular cloning of rare antiviral antibody specificities from phage display libraries. Res. Virol. 149: 327–330.
7. **Burioni, R., P. Plaisant, A. Manzin, D. Rosa, V. Delli Carri, F. Bugli, L. Solforosi, S. Abrignani, P. E. Varaldo, G. Fadda, and M. Clementi.** 1998. Dissection of human humoral immune response against hepatitis C virus E2 glycoprotein by repertoire cloning and generation of recombinant Fab fragments. Hepatology 28:810–814.
8. **Ceray, A., and F. V. Chisari.** 1999. Pathogenesis of chronic hepatitis C: immunological features of hepatic injury and viral persistence. Hepatology 30:595–601.
9. **Kabat, E. A., T. T. Wu, H. M. Perry, K. S. Gottesman, and C. Foeller.** 1991. Sequences of proteins of immunological interest, 5th ed. U.S. Department of Health and Human Services, Bethesda, Md.
10. **Kuo, G., Q. L. Choo, H. J. Alter, G. L. Gitnick, A. G. Redeker, R. H. Purcell, T. Miyamura, J. L. Dienstag, M. J. Alter, C. E. Stevens, et al.** 1989. An assay for circulating antibodies to a major etiologic virus of human non-A, non-B hepatitis. Science 244:362–364.
11. **Lefranc, M. P., V. Giudicelli, C. Ginestoux, J. Bodmer, W. Muller, R. Bontrop, M. Lemaitre, A. Malik, V. Barbie, and D. Chaume.** 1999. IMGT, the international ImMunoGeneTics database. Nucleic Acids Res. 27:209–212.
12. **Lesniewski, R., G. Okasinski, R. Carrick, C. Van Sant, S. Desai, R. Johnson, J. Scheffel, B. Moore, and I. Mushahwar.** 1995. Antibody to hepatitis C virus second envelope (HCV-E2) glycoprotein: a new marker of HCV infection closely associated with viremia. J. Med. Virol. 45:415–422.
13. **Matsuura, Y., H. Tani, K. Suzuki, T. Someya, R. Suzuki, H. Aizaki, K. Ishii, K. Morishii, C. S. Robison, M. A. Whitt, and T. Miyamura.** 2001. Characterization of pseudotype VSV possessing HCV envelope proteins. Virology 286:263–275.
14. **Nunez, J. I., E. Blanco, T. Hernandez, C. Gomez-Tejedor, M. J. Martin, J. Dopazo, and F. Sobrino.** 1998. A RT-PCR assay for the differential diagnosis of vesicular viral diseases of swine. J. Virol. Methods 72:227–235.
15. **Obashi, H., K. Maruyama, Y. C. Liu, and A. Yoshimura.** 1994. Ligand-induced activation of chimeric receptors between the erythropoietin receptor and receptor tyrosine kinases. Proc. Natl. Acad. Sci. USA 91:158–162.
16. **Parren, P. W., P. Fisicaro, A. F. Labrijn, J. M. Binley, W. P. Yang, H. J. Ditzel, C. F. Barbas, and D. R. Burton.** 1996. In vitro antigen challenge of human antibody libraries for vaccine evaluation: the human immunodeficiency virus type 1 envelope. J. Virol. 70:9046–9050.

17. **Rosa, D., S. Campagnoli, C. Moretto, E. Guenzi, L. Cousens, M. Chin, C. Dong, A. J. Weiner, J. Y. Lau, Q. L. Choo, D. Chien, P. Pileri, M. Houghton, and S. Abrignani.** 1996. A quantitative test to estimate neutralizing antibodies to the hepatitis C virus: cytofluorimetric assessment of envelope glycoprotein 2 binding to target cells. Proc. Natl. Acad. Sci. USA 93:1759–1763.

18. **Takada, A., C. Robison, H. Goto, A. Sanchez, K. G. Murti, M. A. Whitt, and Y. Kawaoka.** 1997. A system for functional analysis of Ebola virus glycoprotein. Proc. Natl. Acad. Sci. USA 94:14764–14769.

19. **Takikawa, S., K. Ishii, H. Aizaki, T. Suzuki, H. Asakura, Y. Matsuura, and T. Miyamura.** 2000. Cell fusion activity of hepatitis C virus envelope proteins. J. Virol. 74:5066–5074.